Climate Dynamics (2021) 57:3303–3322
https://doi.org/10.1007/s00382-021-05867-w

Future changes in winter explosive cyclones over the Southern Hemisphere domains from the CORDEX-CORE ensemble

Michelle Simões Reboita[1,2] · Natália Machado Crespo[3] · Jose Abraham Torres[2] · Marco Reale[2,4] · Rosmeri Porfírio da Rocha[3] · Filippo Giorgi[2] · Erika Coppola[2]

Received: 5 March 2021 / Accepted: 24 June 2021 / Published online: 8 July 2021

Abstract
Future projections in austral winter characteristics of explosive extratropical cyclones (EECs) in three CORDEX Southern Hemisphere domains (Africa-AFR, Australia-AUS and South America-SAM) are investigated. The projections are obtained with a fine resolution (25 km) Regional Climate Model (RegCM4) within the CORDEX-CORE framework driven by three Global Climate Models (GCMs: HadGEM2-ES, MPI-ESM-MR and NorESM-1 M) under the RCP8.5 scenario. The cyclone database was obtained using a tracking scheme applied to 6-hourly mean sea level pressure fields and EECs are selected using the Sanders and Gyakum criterion. EECs represent ~ 13–17% of the total number of extratropical cyclones during austral winter in the ERA-Interim reanalysis (1995–2014), while both GCMs and RegCM4 ensembles underestimate this percentage. The frequency of EECs is projected to increase in AFR and in SAM domains at the end of the twenty-first century. However, the magnitude of the projected changes needs to be considered with caution because it is smaller than the underestimations in the frequency of EECs of both ensembles in the present climate. EECs in the future will be deeper and faster but with a shorter lifetime. Eady Growth Rate composites, when EECs reach the explosive phase, indicate a less baroclinic large-scale environment in the future. On the other hand, the intensification of precipitation associated with EECs in the future indicates an increase in the contribution of the diabatic processes acting to strengthen the local baroclinicity of the EECs.

Keywords Explosive extratropical cyclones · Climate change · South America · Africa · Australia · Winds · Precipitation · Eady Growth Rate

1 Introduction

Extratropical cyclones are important synoptic-scale systems often associated with extreme winds and severe precipitation (e.g. Liberato et al. 2011; Reale and Lionello 2013; Gramcianinov et al. 2020) as well as coastal flooding (e.g. Cohen 2011; Lionello et al. 2019, 2020). They can also impact ocean water dynamics down to depths of around 6 km (Kuwano-Yoshida et al. 2016).

Occasionally, some extratropical cyclones experience a fast deepening over a relatively short time period and are, therefore, called explosive extratropical cyclones (EECs) or bombs. According to Sanders and Gyakum (1980), the definition of EECs was firstly introduced by Tor Bergeron, who characterized a rapid deepening of extratropical cyclones as a pressure fall of 24 hPa in 24 h, where this deepening rate is called Bergeron number. As Tor Bergeron mostly focused on cyclones at the latitude of Bergen (~ 60° N), Sanders and Gyakum (1980) adapted the Tor Bergeron's EECs definition for an arbitrary latitude (ϕ) by multiplying the pressure fall rate in 24 h for a correction factor ($\sin(60°)/\sin(\phi)$):

$$\mathrm{NDR} = \frac{\Delta P}{24} \times \frac{\sin(60°)}{\sin(\phi)} \quad (1)$$

where NDR is the so-called Normalised Central Pressure Deepening Rate, Δ P is the variation in the central pressure

✉ Michelle Simões Reboita
reboita@unifei.edu.br

[1] Federal University of Itajubá, UNIFEI, Itajubá, MG, Brazil

[2] Earth System Physics, ESP, The Abdus Salam International Centre for Theoretical Physics, Trieste, Italy

[3] Departamento de Ciências Atmosféricas, Universidade de São Paulo, USP, São Paulo, Brazil

[4] National Institute of Oceanography and Applied Geophysics, OGS, Via Beirut, 2-4, 34151 Trieste, Italy

of the system over a period of 24 h length, ϕ is the latitude of the cyclone center at the midpoint of the 24-h period and 60° is the so-called reference latitude. Thus, NDR = 1 (or 1 Bergeron) is obtained with Δ P ranging from 28 hPa $(24\ h)^{-1}$ at the pole to 12 hPa $(24\ h)^{-1}$ at latitude 25°. By convention, when NDR is equal or higher than one, the system is deemed to be an EEC (Sanders and Gyakum 1980). Sanders (1986) also suggests a classification of EECs in three categories: weak ($1.0 \leq NDR < 1.3$), moderate ($1.3 \leq NDR < 1.8$) and strong ($NDR \geq 1.8$). This classification has been used in studies for the whole hemispheres (Lim and Simmonds 2002; Reale et al. 2019) and in different parts of the world, such as the east Asian coast and northern Pacific (Chen et al. 1992; Yoshida and Asuma 2004), and the southwest South Atlantic Ocean (Bitencourt et al. 2013).

To date, there is no unique theory that fully describes the factors driving the development of EECs. However, it has been suggested that the baroclinic instability in the EECs can be strengthened by different processes: (a) the influence of land/ocean contrasts, since these systems are observed more frequently over the ocean near the east coast of the continents (Danard and Ellemon 1980; Gyakum 1983a, b; Revell and Ridley 1995; Reale et al. 2019); (b) the presence of strong horizontal sea surface temperature (SST) gradients (Sanders and Gyakum 1980; Roebber 1984; Sanders 1986; Carlson 1991; Cione and Raman 1995); (c) the effect of latent and sensible heat fluxes from the ocean to the atmosphere (Sanders and Gyakum 1980; Nuss and Anthes 1987; Rogers and Bosart 1991; Kuo and Reed 1988; Uccellini 1990; Rogers and Bosart 1991; Wash et al. 1992; Crescenti and Weller 1992; Neiman and Shapiro 1993; Zhang et al. 1999; Piva et al. 2011); (d) moist diabatic processes such as the latent heat release by cloud condensation processes (Dias Pinto e da Rocha 2011; Fink et al. 2012; Willison et al. 2013); (e) superposition of the jet maximum quadrant and its associated divergence over the surface cyclone (Uccellini and Kocin 1987); and (f) a combination of the aforementioned multiple factors (Bullock and Gyakum 1993; Nesterov 2010; Heo et al. 2019; Reis et al. 2020; Schossler et al. 2020).

Sanders and Gyakum (1980) showed that EECs in the Northern Hemisphere (NH) develop over a wide range of SST, from 0° to 23 °C, indicating that these systems are not as sensitive to SST as tropical cyclones. The most important factor for the development of EECs is the temperature contrast between the surface of the ocean and the atmosphere, which causes intense latent and sensible heat exchanges when dry, cold continental air passes over a relatively warm ocean surface (Neiman and Shapiro 1993). This exchange is more intense in winter, when the ocean is relatively warmer than the atmosphere, and for this reason, climatological studies show that EECs are also more frequent in winter (e.g., Chen et al. 1992; Lim and Simmonds 2002; Allen et al. 2010; Bitencourt et al. 2013; Zhang et al. 2017; Reale et al. 2019). According to Nuss and Anthes (1987) and McMurdie and Houze (2006), when the transfer of energy from the ocean to the atmosphere is maximum in the warm sector of the cyclones, the horizontal temperature gradient of these systems is strengthened, which increases the supply of potential energy available to be converted into kinetic energy and results in an intensification of the cyclone.

Shapiro and Keyser (1990) showed that not all extratropical cyclones over the ocean follow the conceptual model of Bjerknes and Solberg (1922), i.e., instead of the cold front rotating into the warm front, the cold front fractures from the warm front and moves perpendicularly to it. According to Cohen (2011), the roughness of the Earth's surface may affect the types of frontal structures: land (ocean) has higher (lower) friction and favours cyclones of the Bjerknes and Solberg type (Shapiro and Keyser model). An interesting feature in the Shapiro and Keyser model is that there is warm seclusion in the cyclone center, which resembles the eye of tropical cyclones (Cohen 2011).

Since the paper by Sanders and Gyakum (1980), several other studies focused on EECs climatologies, either covering whole hemispheres (Sinclair 1995; Lim and Simmonds 2002; Allen et al. 2010; Eiras-Barca et al. 2018; Reale et al. 2019; Fu et al. 2020) or limited areas such as the southwest South Atlantic (Bitencourt et al. 2013); southwest Pacific (Leslie et al. 2005; Black et al. 2010); Mediterranean Sea (Kouroutzoglou et al. 2011), east Asia (Chen et al. 1992), west of northern Pacific (Chen and Lu 1997), and the northern Pacific (Zhang et al. 2017). Lim and Simmonds (2002) modified Eq. (1) to account for "spatial changes of background (or climatological) pressure along the cyclone path", i.e., they changed P in Eq. (1) to PR, where PR is the difference between the central pressure of a cyclone and the climatological pressure at the cyclone location at that time of year. Using the NCEP-DOE reanalysis for the period 1979–1999, they obtained an average of 26.4 EECs $year^{-1}$ in the Southern Hemisphere (SH), with ~ 40% of these systems occurring in winter. Moreover, EECs represent less than 1% (0.5%) of the winter (summer) total cyclone population in the SH. Using the classification of Sanders (1986), Lim and Simmonds (2002) found a higher frequency of weak EECs (87%) in the SH, with only a rare occurrence of strong EECs.

Allen et al. (2010) constructed a global climatology of EECs considering four reanalysis datasets covering the period 1979 to 2008, and three methods for EECs classification: (a) Sanders and Gyakum (1980), (b) Lim and Simmonds (2002), and (c) a combined method where the system needs to fit both (a) and (b) conditions, which avoids the inclusion of artificial EECs identified by Lim and Simmonds (2002). In the ERA-Interim reanalysis, the annual number of EECs in the SH can range from 31 (combined method of Allen et al. 2010) to 171 (Sanders and Gyakum

method). Recently, Reale et al. (2019) applied the Sanders and Gyakum (1980) definition to the ERA-Interim reanalysis (1979–2009). For the SH, the authors obtained an annual average of 187 EECs, representing 11% of the total cyclone number. The difference in the EEC climatologies by Reale et al. (2019) and Allen et al. (2010) is due to the different algorithms applied to detect and track the cyclones. For the southwestern South Atlantic Ocean (45° S–15° S and 60° W–20° W), Bitencourt et al. (2013) found an annual mean varying from 1.57 using Lim and Simmonds (2002) to 2.7 using the Sanders and Gyakum (1980) method, which represents 2.4% and 4.1% of the total cyclone climatology, respectively.

In the SH, EECs preferentially occur (a) over the Southern Ocean surrounding Antarctica and southeast South America (mainly off the coast of Uruguay), (b) over a band extending across the Southern Atlantic and Indian oceans (near south and southeast Africa), (c) east of the Australian continent and New Zealand (Tasman Sea), and (d) in the South Pacific Ocean (Sinclair 1995; Allen et al. 2010; Cohen 2011; Bitencourt et al. 2013; Reale et al. 2019). EECs that form close to Southern Africa and Australia are usually faster and with a higher deepening rate than those close to South America (Reale et al. 2019). On the other hand, EECs forming close to South America and Africa are characterized by a higher normalized deepening and duration (Reale et al. 2019).

Positive trends in the annual frequency of EECs in the SH have also been documented. Lim and Simmonds (2002) obtained an increase of 0.56 EECs year^{-1} from 1979 to 1999, while Reale et al. (2019) found an increase of 0.4 EECs year^{-1} from 1979 to 2008. Allen et al. (2010) also observed an increase in the frequency of rapidly intensifying systems during the period 1979–2008, consistently with other studies including total cyclone climatologies (Reboita et al. 2015, 2020; Kodama et al. 2019).

Studies focusing on the EECs in future climate scenarios are still scarce. A few studies using global climate models (GCMs) include Chang et al. (2012) and Kodama et al. (2019), who focused on both the NH and SH, Seiler and Zweirs (2016a; b; NH only) and Chang (2017; SH only). It is worth mentioning that Chang et al. (2012), Chang (2017), and Kodama et al. (2019) do not apply the classical EECs definition in their studies and for this reason, the cyclones are simply called intense. Chang et al. (2012) analyzed 23 Coupled Model Intercomparison Project Phase 5 (CMIP5) GCMs under the Representative Concentration Pathway 8.5 (RCP8.5) scenario and found a significant increase in the frequency of EECs during the cold season in the SH, along with a significant decrease in the NH. Similar trends, but without statistical significance, were observed by Kodama et al. (2019) in a simulation under the A1B scenario. Seiler and Zweirs (2016a) evaluated the performance of CMIP5 GCMs in simulating the EECs from 1980 to 2005 in the NH and found that the models tend to simulate too few and weak explosive EECs compared to ERA-Interim. They also found a northward shift of about 2.2° latitude in the distribution of EECs associated with a poleward shift of the jet stream by the end of the twenty-first century (RCP8.5). This coupling between EECs and the jet stream is explained through the mass divergence at upper levels, which occurs in the jet streak (higher wind intensity) regions and at the right side of the troughs in the meandering flow, with consequent lowering of pressure at low levels. In the Atlantic Ocean, they also observed a decrease of 17% in the number of EECs and a small increase in their intensity. The reduction in the EEC frequency south of 45°N is coincident with a decline in the lower-tropospheric Eady Growth Rate and an increase in static stability.

Differently from the NH, Chang et al. (2012) and Chang (2017) show a positive trend of intense systems in the SH at the end of the century from 26 CMIP5-GCMs under the RCP8.5 scenario. Chang (2017) also shows a poleward displacement of the most extreme cyclones. These results are in line with those from Reboita et al. (2020), who show a decrease in the frequency of the total cyclones over the SH and an increase in the number of the intense systems under the RCP8.5 scenario in projections with GCMs and the Regional Climate Model version 4 (RegCM4). Regional Climate Models (RCMs) are indeed an important tool for studying EECs since they can resolve better their mesoscale structures due to their relatively high horizontal resolution (Kuwano-Yoshida and Asuma 2008; Bader et al. 2011; Willison et al. 2013; Michaelis et al. 2017; Seiler et al. 2018; Ambrizzi et al. 2019). For example, Willison et al. (2013) show a positive feedback between cyclone intensification and latent heat release in higher resolution simulations compared to coarser resolution ones, resulting in stronger cyclones.

In terms of EEC projections with RCMs, to the best of the authors' knowledge, there is only one study available, which focuses on the North America Atlantic coast (Seiler et al. 2018) with CanRCM4 forced with the CanESM2 GCM. It was shown that CanESM2 underestimates by 38% the EECs over the region, while CanRCM4 ameliorates this underestimation (22%) and the associated precipitation. Under the RCP8.5 scenario, both the GCM and RCM project a decrease in EEC frequency (− 15%, − 18%) and Eady Growth Rate (− 0.2 day^{-1}, − 0.2 day^{-1}), and an increase in precipitation (46%, 52%).

From this literature review, it appears that there are no RCMs based studies of EECs in the SH within a climate change context. The recent completion of a new ensemble of RegCM4 projections (Reboita et al. 2020) within the framework of the CORDEX-CORE initiative (Gutowski et al. 2016) offers the opportunity to revisit this issue in a

multi-domain context, since this ensemble includes three domains extending to the extratropical SH (Africa, Australia and South America). The projections extend from 1970 to 2100 and are driven by multiple GCMs from the CMIP5 ensemble. Although two scenarios were simulated, the low-end RCP2.6 and high-end RCP8.5 scenario, here we focus on the latter one to maximize the magnitude of the change signal. The RCM adopted here is the RegCM4 (Giorgi et al. 2012) developed at the Abdus Salam International Centre for Theoretical Physics (ICTP), and the focus is on the austral winter (June–July–August). In the next section, we begin with a description of models, simulation protocol, and analysis methodology.

2 Methodology

2.1 Climate projections

The cyclone database used in this study is based on the application of an automatic detection and tracking scheme to the 6-hourly Mean Sea Level Pressure (MSLP) fields produced by RegCM4 and the driving GCMs. Here, we briefly describe the climate projections and the method applied to detect and track cyclones, while a complete description of both is already provided in Reboita et al. (2020) and references therein.

RegCM4 is a participant of the CORDEX-CORE initiative (Coordinated Regional Downscaling Experiment (CORDEX)—Coordinated Output for Regional Evaluations (CORE); Gutowski et al. 2016) under which a new ensemble of RCM-based projections was completed for a number of domains defined by the CORDEX program (Giorgi et al. 2009). In order to provide projections for the three SH domains from CORDEX (Africa—AFR, Australia—AUS and South America—SAM; Fig. 1), and following the CORDEX-CORE protocol (Teichmann et al. 2021), RegCM4 was nested in three GCMs from CMIP5: the Hadley Center Global Environment Model version 2 (HadGEM2-ES, Collins et al. 2008), the Max Planck Institute Earth System Model (MPI-ESM-MR, Giorgetta et al. 2013), and the Norwegian Earth System Model (NorESM-1 M; Bentsen et al. 2013). The choice of these GCMs was based on their relatively good performance over the CORDEX-CORE regions and the fact that they roughly span the range of climate sensitivities in the CMIP5 ensemble (Teichmann et al. 2021).

Projections were carried out at 25 km horizontal grid spacing and 23 sigma-pressure levels. The emission scenario adopted is RCP8.5. Following the Intergovernmental Panel on Climate Change (IPCC) recommendation for AR6, we analyze the reference period 1995–2014 (hereafter historical period) and the end-of-century period 2080–2099 (hereafter far-future period). For AFR only two projections are available: RegCM4 nested in HadGEM2-ES and in NorESM-1 M, therefore, for this domain, we also consider only two GCMs projections in the analysis.

2.2 Cyclone detection and tracking

The cyclone detection and tracking method (CDTM) developed by Lionello et al. (2002) and Reale and Lionello (2013) was applied to 6-hourly MSLP fields produced by RegCM4, the GCMs and the ERA-Interim reanalysis (ERAI; Dee et al. 2011). All model data were interpolated onto the ERAI grid ($0.75° \times 0.75°$) before applying the tracking scheme. Based on previous studies (Neu et al. 2013; Lionello et al. 2016; Reale et al. 2019; Reboita et al. 2020), only ERAI is used to validate the simulated EECs. However comparisons with a single reanalysis should be carried out with caution since some differences have been observed among reanalysis in terms of cyclones' frequency, inter-annual variability etc.

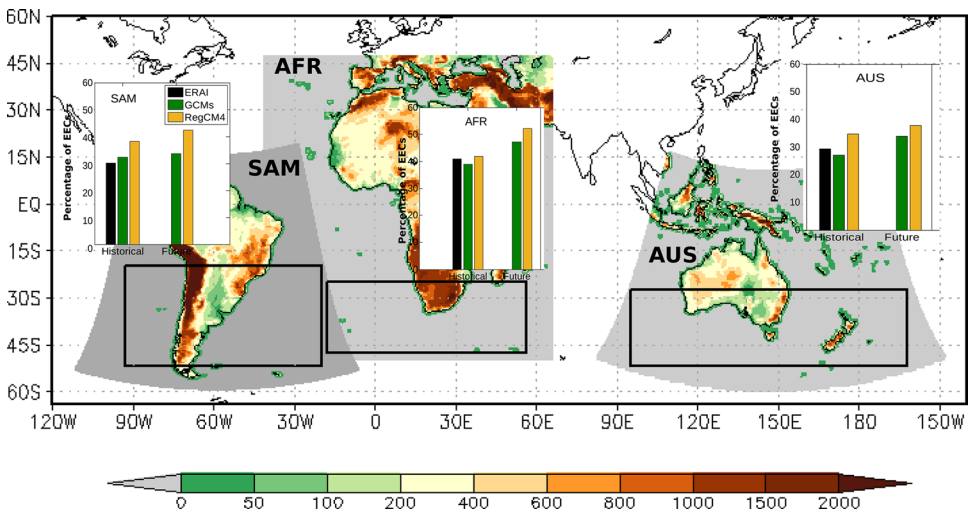

Fig. 1 Domain (grey areas) and topography (m) of the simulations, tracking area (black boxes) and relative contribution (%) of the EECs in JJA to the annual total of EECs in the historical and future climate.

(e.g. Di Luca et al. 2015; Crespo et al. 2020a; Marrafon et al. 2021).

The CDTM has already been applied to GCMs and RCMs data in different comparison studies belonging to the Intercomparison of MId LAtitude STorm Diagnostics project (IMILAST; Neu et al. 2013; Ulbrich et al. 2013; Lionello et al. 2016, 2019; Flaounas et al. 2018; Reale et al. 2019, 2021; Reboita et al. 2020). CDTM provides the central position (latitude and longitude), MSLP minimum (in hPa), Laplacian (in hPa m^{-2}) and depth (hPa) of a cyclone at each time step of its lifecycle. The depth of each system is obtained as the difference between the MSLP background field and the MSLP minimum at the center of the cyclone (Reale and Lionello 2013). As in Reboita et al. (2020), here we consider only systems with a lifetime equal or higher than 24 h reaching a depth equal or higher than 10 hPa during their lifecycle.

2.3 EEC classification

As in previous studies (Kouroutzoglou et al. 2011; Seiler and Zweirs 2016a, b; Eira-Barcas et al. 2018; Reale et al. 2019; Schossler et al. 2020), here EECs are identified using the original formulation of Sanders and Gyakum (1980; Eq. 1). Although the original formulation of Sanders and Gyakum (1980) is still widely used in recent studies (Reale et al. 2019), it has the limitation of not capturing properly those systems that rapidly deepen over periods shorter than 24 h and then quickly weaken before the 24-h mark. For instance, if a cyclone deepens by 24 hPa in 20 h but then slightly weakens by 1 hPa at the 24-h mark (such that it deepened by 23 hPa over 24 h), it would not be considered explosive by Sanders and Gyakum (1980) formulation even though it was characterized by relatively high deepening rate. Similarly, if a cyclone deepens by 28 hPa in 18 h but then weakens by 2 hPa by the 24-h mark (such that it deepens by 26 hPa in 24 h) it would appear less explosive than it actually was using this measure. Here, we adopted the Sanders-Gyakum definition to allow a fair intercomparison of our results with those available in the scientific literature. An evaluation of the sensitivity of the EECs climatology and climate change signal with respect to different detection criteria is a very interesting point for a next investigation.

The EEC dataset also follows the IMILAST project protocol (Neu et al. 2013). Initially, the first period of 24 h within the cyclone lifecycle (five time steps) is considered. To compute the change of pressure during this period, the first cyclone position (index $1 = t_0$) is subtracted from the fifth position (index $5 = t_{24}$), as shown in Eq. (2). In the next iteration, t_{24} and t_0 become indices 6 and 2 and so on. In Eq. 2 we maintain the sine factor with positive values and multiply the NDR by –1 in order to obtain NDR > 1 for EECs.

$$\mathrm{NDR}\left(t_{24}\right) = -1 \times \left(\frac{MSLP(t_{24}) - MSLP(t_0)}{24}\right) \times \frac{\sin(60°)}{\sin\left(\frac{|lat(t_{24})|+|lat(t_0)|}{2}\right)} \quad (2)$$

2.4 Analyses

Once the EECs in each GCM and RegCM4 member are identified, ensemble averages are computed for the austral winter frequency, trend, mean intensity, lifetime and travelled distance of these systems. Selecting their maximum value of NDR along the lifecycle, EECs are also classified as weak ($1.0 \leq \mathrm{NDR} < 1.3$), moderate ($1.3 \leq \mathrm{NDR} < 1.8$) and strong ($\mathrm{NDR} \geq 1.8$) following Sanders (1986).

In order to evaluate the changes in the environmental background of EECs, we compute the composites of MSLP, precipitation, winds at 850 hPa and the Eady Growth Rate (EGR) at 850–500 hPa layer, which is an indicator of the large scale baroclinicity, for each domain, time slice and ensemble. The EGR describes how well synoptic pressure systems can develop in a given weather situation over a specific area (Hoskins and Valdes 1990). More specifically, it allows a quantification of the baroclinic instability of the environment, since it depends on the vertical wind shear (which is associated with the meridional temperature gradient) and the static stability N (also called Brunt–Väisälä frequency):

$$EGR = 0.31 \frac{|f|}{N}\left|\frac{\delta v}{\delta z}\right| \qquad with \qquad N = \left(\frac{g}{\theta}\frac{\delta\theta}{\delta z}\right)^{\frac{1}{2}} \quad (3)$$

where f is the Coriolis parameter, g is the gravity acceleration ($m\ s^{-2}$), v is the horizontal wind speed ($m\ s^{-1}$), z is geopotential height (m) and θ is the potential temperature (K). The physical interpretation of the EGR is that air parcels displacing in a slope produced by a horizontal temperature gradient have a lower center of gravity while at the same time the buoyancy effects can allow the parcels to continue to move. Then, there is release of available potential energy and a gain of kinetic energy by the disturbance (Schartner and Kirchner 2016).

The composites consider two specific EECs time steps: genesis and explosive phase. For composites calculation, an area of 30° in longitude by 20° in latitude centered in the cyclone center was selected. The center of each system is given by the lon-lat coordinates provided by the tracking scheme. The selected data are then averaged to provide a mean synoptic field for each variable at the genesis or explosive time. Here it is important to stress that the axes of the maps obtained do not indicate the actual coordinate of each cyclone but the distance in degrees in all the directions from the center of the cyclone.

Since precipitation and geopotential height are available at a daily frequency in the GCMs, in order to standardize our analysis, daily data of these variables are used in the composite of both GCMs and RegCM4. For the other variables, the 1200 UTC time is selected. Since RegCM4 has a limited area, many cyclones, especially during the explosive phase, are located very close to the border. Therefore, to avoid discontinuities in the composite fields, we selected EECs with centers lying at least 5° in each direction from the domain boundary. Finally, the central MSLP is defined as the smallest value in the cyclones center composite (Table S1) that can be different from the most central isobar.

3 Results

3.1 EEC frequency

Approximately 40% of the annual total of EECs occurs in JJA in the AFR domain and approximately 30% in the AUS and SAM domains (Fig. 1). These relative contributions shown by ERAI are also generally simulated by the historical simulations (although with some differences) and are consistent with the value of ~ 40% found by Lim and Simmonds (2002) considering the entire SH. RegCM4 in the three domains overestimates the percentage found in ERAI while the GCMs ensemble underestimates it in AFR and AUS and overestimates it in SAM (Fig. 1). The JJA percentage of EECs increases in the future climate compared to the present (Fig. 1) as a consequence of two factors: the projected decrease of the total number of cyclones and the increase of the number of EECs (which we can see for the austral winter in Table 1).

From Table 1 we highlight that the ensembles underestimate the frequency of the total number of cyclones (EECs and non-EECs) in JJA compared to the ERAI with consequent underestimation of the frequency of EECs. The highest underestimation in the total number of cyclones is registered in the GCMs (28% and 24% respectively) in AFR and SAM and in the RegCM4 (33%) in AUS.

In terms of EECs, GCMs also have the highest underestimation, both in SAM (47%) and AUS (58%) domains. Although RegCM4 has better results, the underestimates are also large (Table 1). The proportion of EECs by the total number of cyclones (EECs/total) in each domain represents ~ 13–17% in ERAI during the austral winter, while the two ensembles, in general, tend to underestimate this value. The ERAI relative frequency of EECs is slightly higher than obtained by Reale et al. (2019), which may also be attributed to the fact that here we analyze limited area domains, while Reale et al. (2019) considered the whole SH. In the AUS and SAM domains, the percentage of EECs in RegCM4 is closer to the ERAI values than that of the GCMs, while the opposite is found in the AFR domain (Table 1).

The underestimations of the ensembles can be traced back to the absence of data assimilation and low temporal and spatial resolution of GCMs, which makes it difficult to solve some cyclones and decrease the number of simulated systems. This also limits the numbers of systems simulated by RegCM4, as most systems simulated by the limited area models originate outside the domain itself and enter into the domain through the boundary conditions (Reale et al. 2021). Moreover, if a system simulated by the GCM moves too fast it could cross the domain boundaries without leaving a fingerprint in the relaxation zone, it becomes completely missed in the RegCM4 simulated climatologies (Sanchez-Gomez and Somot 2018; Reale et al. 2021). This points out the importance of the numerical settings in RCMs as a source of possible difference between references and simulated regional datasets. Despite the biases in the

Table 1 Ensemble of the total of cyclones (EECs and non-EECs) and EECs in the three Southern Hemisphere domains in the historical (1995–2014) and future climate (2080–2099) during JJA

DATA	Historical			Future		
	Total	EECs	%	Total	EECs	%
AFR						
ERAI	159.0	27.0	17.0			
GCMs	114.5	14	12.2	114.0	17.7	15.5
RegCM4	139.0	8.0	5.8	123.5	12.0	9.7
AUS						
ERAI	522.0	68.0	13.0			
GCMs	433.3	28.3	6.5	329.7	34.3	10.4
RegCM4	351.0	30.0	8.5	285.0	29.0	10.2
SAM						
ERAI	351.0	58.0	16.5			
GCMs	264.7	30.7	11.6	221.3	42.0	19.0
RegCM4	270.0	36.3	13.4	230.3	44.7	19.0

The percentage (%) indicates the percentage of EECs regarding the total number of cyclones

frequency of total cyclones, Reboita et al. (2020) discussed that the RegCM4 and GCMs ensembles are able to simulate the mean characteristics and key related variables of the cyclones in the present climate. Here, we also show that the simulated EECs capture the main features of the ERAI (Sect. 3.3), although the proportion of EECs/total is, in general, underestimated by both GCMs and RegCM4 compared to ERAI (Table 1).

Comparing the frequency of EECs in the future and present climates, both ensembles indicate an increase in the frequency of these systems, except for RegCM4 in AUS domain (Table 1). In this case, the highest increase is projected to AFR by RegCM4 (33%). Our result is in line with Chang (2017), who found an increase in the number of intense cyclones in future warmer conditions. Another way to evaluate the changes of EECs is comparing the proportion of EECs/total in the future and present climates. Following this analysis, the largest increase is projected over the SAM domain (7.4% in the GCMs and 5.6% in RegCM4), then by AFR (3.3% in GCMs and 3.9% in RegCM4) and AUS (3.9% in GCMs and 1.7% in RegCM4). However, this increase is not statistically significant at $\alpha = 0.05$.

Although the sign of the projected changes in the frequency of EECs is consistent with those discussed in the scientific literature (e.g. Chang et al. 2012; Seil et al. 2018), their magnitude needs to be considered with caution. From Table 1, for the present climate, EECs in ERAI represent ~ 13–17% of the total number of extratropical cyclones detected in each domain, while in RegCM4 this proportion is 5.8% for AFR, 8.5% for AUS and 13.4% for SAM. While RegCM4 does better the proportion of EECs in the SAM domain (bias of 19%), there is a larger bias in AFR (66%) and AUS (35%). For the future climate, Table 1 shows that RegCM4 ensemble projects an increase of 19% for AFR and 33% for SAM in the frequency of EECs, while no changes have been identified in AUS. Thus, the magnitude of the projected changes is smaller than the RegCM4 underestimation of EECs in the present climate. This limits the confidence in the magnitude of the future changes of EECs, not on their signs which are consistent with those discussed in the scientific literature.

While Table 1 indicates a future increase in ECC frequency, Fig. 2 shows that this increase is not statistically significant at $\alpha = 0.05$, which implies that it could also be due to a large interannual and interdecadal variability (Fig. 2), or in other words, there are no positive trend lines.

3.2 EC density

The spatial distribution of EECs in ERAI over the SAM domain shows that the region encompassing southern Brazil and Uruguay is the preferential location for explosive cyclogenesis (shaded color in Fig. 3a) and that these systems reach the EEC category south or southeast of the genesis area (continuous lines in Fig. 3a). The extreme south of Brazil and Uruguay is one of the three main cyclogenetic regions near the South America coast and it is more active during the austral winter (Hoskins and Hodges 2005; Reboita et al. 2010, 2015; Crespo et al. 2020b), with cyclogenesis being associated with the lee effect, troughs travelling from the Pacific to the Atlantic Ocean, and meridional thermal contrasts near the surface (Gan and Rao 1991; Seluchi 1995; Vera et al. 2002; Hoskins and Hodges 2005; Reboita et al. 2012, 2018). Over the AFR domain, the EECs main genesis region lies far from the continent in the latitude band 40°–50°S, which is also the band of higher EECs frequency in the AUS domain. Cyclogenesis in this latitude band is associated with the intense horizontal temperature gradients, which are a typical feature of these latitudes (Holton 2004). AUS also has EEC cyclogenesis near the southeast of the continent, 30°–40°S (same latitude band of the maximum of EECs in the SAM), with the source of this signal a matter of debate in the scientific literature (see Pepler et al. 2017).

In all domains, the model ensembles reproduce the spatial distribution of EECs found in ERAI (Fig. 3a–c). RegCM4 improves the GCMs results over the SAM domain, where it shows higher EECs density near the extreme south of Brazil and Uruguay. For the future climate (Fig. 3d–g), both ensembles project an increase in the number of EECs near the coast of southern Brazil and Uruguay, but these systems reach the EEC category far from the coast, with some cases displaced more northwards in RegCM4. Despite the noisy change signal in AFR and AUS, both ensembles indicate a tendency for increased numbers of EECs. Figure 3f–g also suggests that south of 40°S in the future, cyclones reach the EEC category with a poleward displacement, a feature that is more evident in the RegCM4 ensemble for the AUS domain. A southward displacement of intense cyclones in the future climate was also found by Chang (2017).

3.3 Mean EEC features

The main climatological features of the EECs in each domain, ensemble, and timeslice are shown in Fig. 4. The model ensembles are able to reproduce the frequency distributions of the EECs as found in ERAI and, in general, RegCM4 has a better performance than the GCMs. Some examples are the maximum depth in the AFR domain (Fig. 4a), the minimum pressure in the three domains (Fig. 4g–i), and the lifetime in the AUS and SAM domains (Fig. 4k–l).

Note that, while Reboita et al. (2020) found the highest frequency of cyclones with a maximum depth of ~ 30 hPa in the total climatology of winter systems, our analysis indicates that EECs have a higher frequency with depth of ~ 50 hPa (Fig. 4a–c). More specifically, AFR and

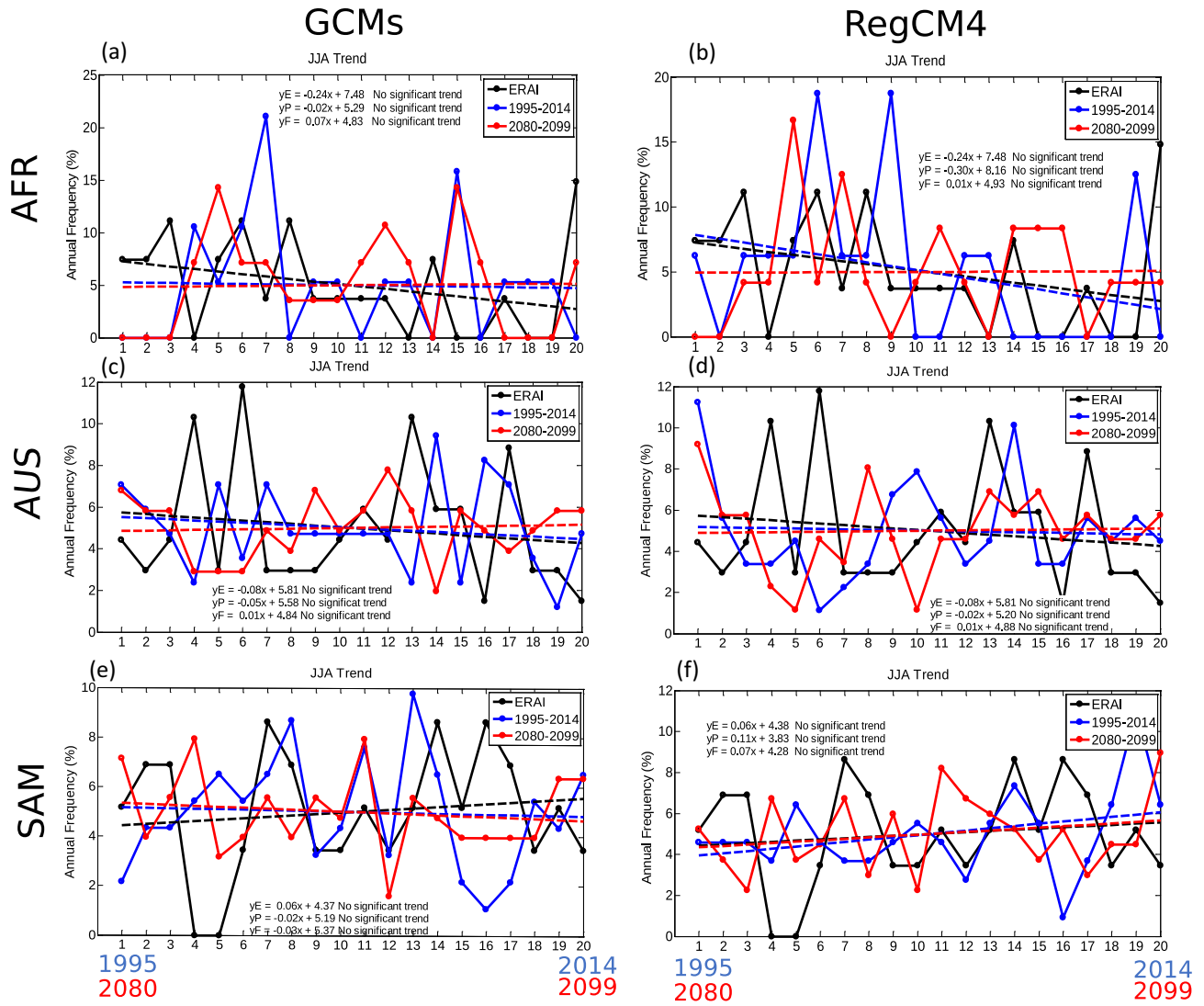

Fig. 2 EECs standardized frequency in JJA, i.e., the number of EECs in JJA of each year divided by the total number of EECs of austral winter considering the whole studied period. Black lines indicate ERAI, blue lines the ensembles in the present climate and red lines the ensembles in the future climate. GCMs (RegCM4) ensemble is presented on the left (right) side. All panels show the equations of the linear trend that are represented in dashed lines. The horizontal axis corresponds to the years, which range from 1995 to 2014 in the historical climate and from 2080 to 2099 in the future climate

AUS show a higher percentage of systems with depth of 50–60 hPa, while SAM has a maximum with depth of 40–50 hPa. Similar results were obtained by Reale et al. (2019) for a present climate study. We suggest that in SAM the depth is lower because the systems originate in the subtropics, a region less baroclinic than mid-latitude (Fig. 3). During the time that the cyclones reach the EEC category (Fig. 4d–f), the depth is almost 10 hPa lower (~40 hPa) than the maximum depth (~50 hPa) reached by EECs. The mismatch between the two values can be explained by the fact that here we are comparing the maximum depth at the time the system is deemed as explosive and the maximum depth along its lifecycle. In fact, once the system has become explosive the deepening process can still continue resulting in depth even stronger than at the time of explosive deepening.

Another measure of cyclone intensity is the minimum pressure found during the EEC lifecycle (Fig. 4g–i). In the three domains, the highest frequency of EECs is found when the minimum central pressure ranges from 960 to 970 hPa. Concerning the climate change signal, in all domains, the ensembles show an increase in the frequency of the EECs with higher depth and lower central pressure, but this signal is not statistically significant ($\alpha = 0.05$). The frequency distributions of the minimum pressure show that GCMs tend to simulate deeper cyclones than RegCM4 and ERAI.

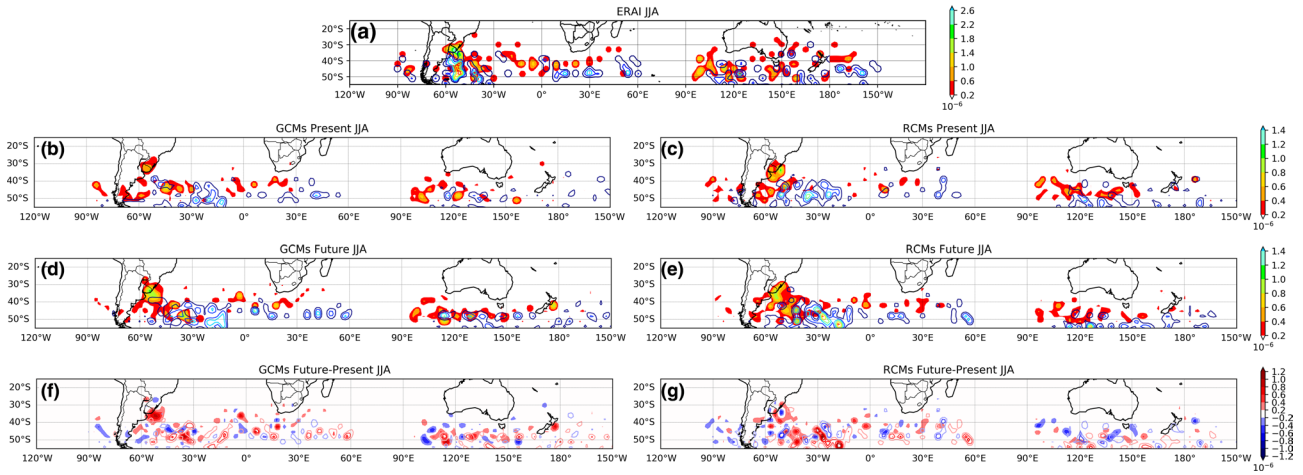

Fig. 3 EECs density [(number of systems in regions of 3°×3° per area (km^2))×10^6] in two-time steps: cyclogenesis (shaded) and when the cyclones reach the explosive category (continuous lines: **a**–**e** from 0.2 to 3.0, 0.4 interval and **f**, **g** same interval as for cyclogenesis). **a** ERAI, **b** GCMs ensemble and **c** RegCM4 ensemble in the historical period; **d**, **e** in the RCP8.5 scenario and **f**, **g** the differences between future (2080–2099) and historical period (1995–2014). A statistical significance test was not included in figures f and g since it tends to be very patchy as a function of high time–space variability of the cyclones (Pezza et al. 2012)

The same behaviour is not observed in studies of tropical cyclones (e.g., Tonkin et al. 2000; Suzuki-Parker 2012; Wang et al. 2017; Davis 2018), suggesting that extratropical cyclones do not have the same horizontal resolution dependency as that seen for tropical cyclones. In fact, as discussed by Gentry and Lackmann (2010), the only way for a model or a reanalysis to reproduce with a certain degree of accuracy the minimum pressure in a tropical cyclone would be adopting a resolution of a few kilometers, which is computationally expensive and thus not considered until now in the climate simulations. Moreover, tropical cyclones usually have smaller spatial scales and thus low-resolution models are less prone to simulate their dynamics. On the other hand, as discussed in the introduction, baroclinic and diabatic processes can drive the intensity of a simulated extratropical cyclone. Additionally, several factors associated with the configuration of the models (such as physical parameterization schemes) may play a role in the intensity of the extratropical cyclones through the changes in the vertical stability, moisture flux and moisture content in the atmosphere, convection representation, wind divergence at the upper levels just to cite a few. In our analysis, GCMs tend to simulate deeper cyclones over some domains due to a combination of the aforementioned factors. However, the analysis of these factors would require a deeper work only focused on the GCMs ensembles and it is beyond the scope of this study.

In present climate conditions, the highest frequency of cyclones becomes explosive in the first 24 h after cyclogenesis (Fig. 4m–o) and when they last more than 48 h (Fig. 4j–l). The EEC duration is higher compared to that of all cyclones (24–48 h; Reboita et al. 2020). Moreover, the AUS domain shows a higher frequency of EECs lasting between 144 to 240 h than the AFR and SAM, which can be associated with the longer distances travelled by EECs in AUS (Figure not shown) and it is a similar feature shown in Reale et al. (2019). In future conditions, in AFR and SAM (Fig. 4j, l) there is an increase in the frequency of cyclones lasting less than 48 h in RegCM4, which is not generally noted in GCMs. In AUS (Fig. 4k), this increase occurs in both ensembles.

The mean speed frequency distribution of EECs in the present climate time slice (Fig. 4p–r) resembles that of all cyclones climatology presented in Fig. 5 by Reboita et al. (2020), where most cyclones have a mean speed in the range of 6–12 m s^{-1}. In the future, however, RegCM4 indicates a decrease in the frequency of slow EECs and an increase of EECs with a mean speed higher than 15 m s^{-1} over all domains.

In summary, in present climate conditions, EECs are deeper and longer-lasting compared to all cyclone climatology, and in future warmer conditions, the projections indicate deeper and faster EECs with a shorter lifetime, although these results are mostly not statistically significant ($\alpha = 0.05$).

3.4 Sander's classification

EECs are classified according to Sander's methodology in three categories: weak ($1.0 \leq NDR < 1.3$), moderate ($1.3 \leq NDR < 1.8$) and strong ($NDR \geq 1.8$). In the AFR domain, ~ 50% of the EECs in ERAI are weak systems, while in AUS and SAM this percentage is around 60%. Although both ensembles overestimate the frequency of weak EECs

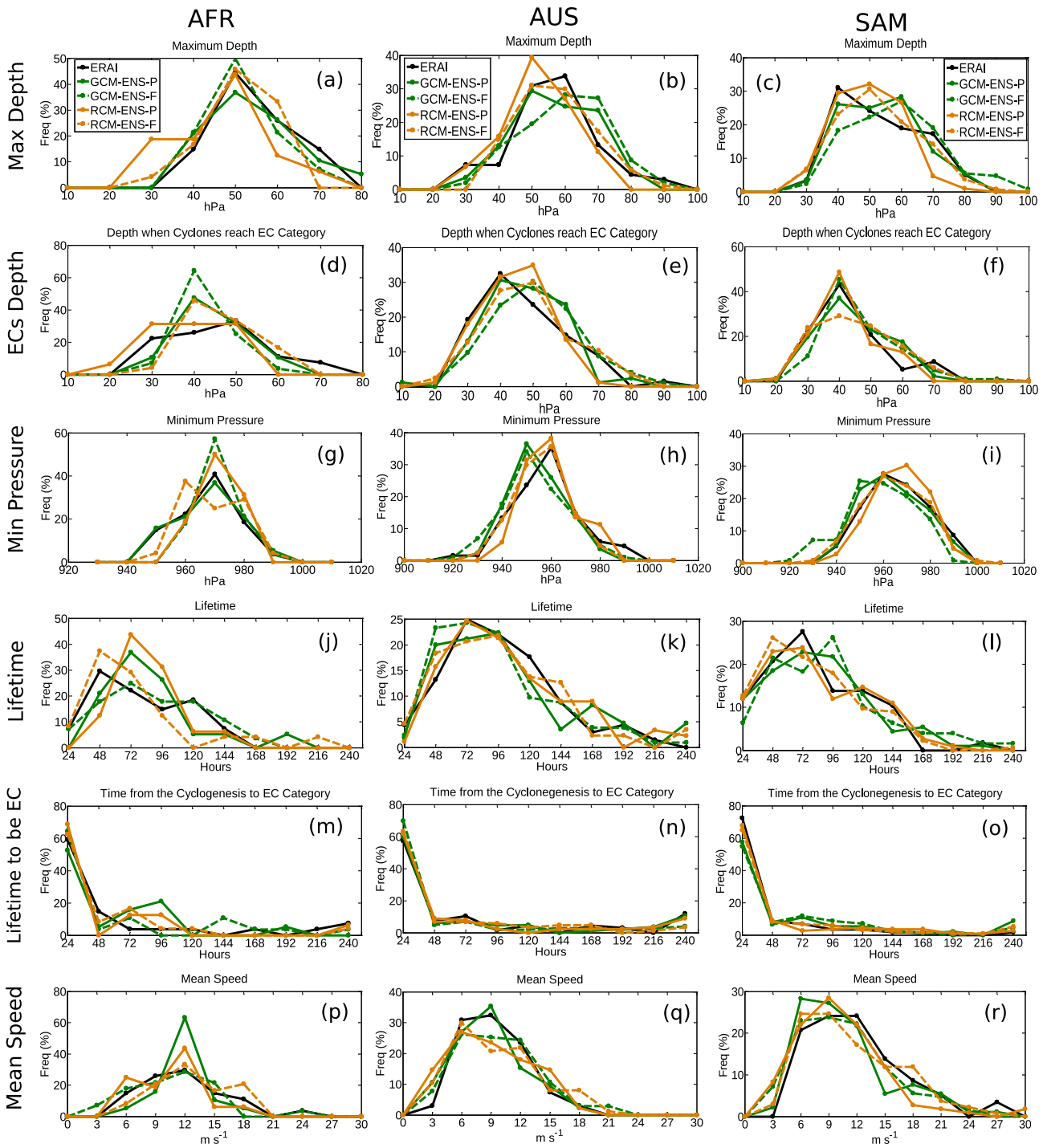

Fig. 4 Frequency distribution of **a**–**c** the maximum depth occurred in the EECs lifecycle (hPa), **d**–**f** depth when the cyclones reach the EEC category (hPa), **g**–**i** minimum sea level pressure occurred in the EECs lifecycle (hPa), **j**–**l** lifetime (hour), **m**-**o** lifetime from cyclogenesis to EEC category (hour), and **p**–**r** mean speed (m s^{-1}) of the EECs occurred in JJA in the GCMs (green) and RegCM4 (orange) ensembles in the present (ENS-P; continuous line) and future climate (ENS-F; dashed line). ERAI is shown in black line

and underestimate the moderate ones (Fig. 5), RegCM4 shows a better performance than the GCMs. In terms of strong systems, the percentage is near 15% in SAM and almost zero in AUS. In the future, in AUS and SAM, the number of weak EECs is projected to decrease, while the number of moderate ones, to increase. In AFR, RegCM4 indicates a slight increase in weak EECs and a decrease in moderate ones.

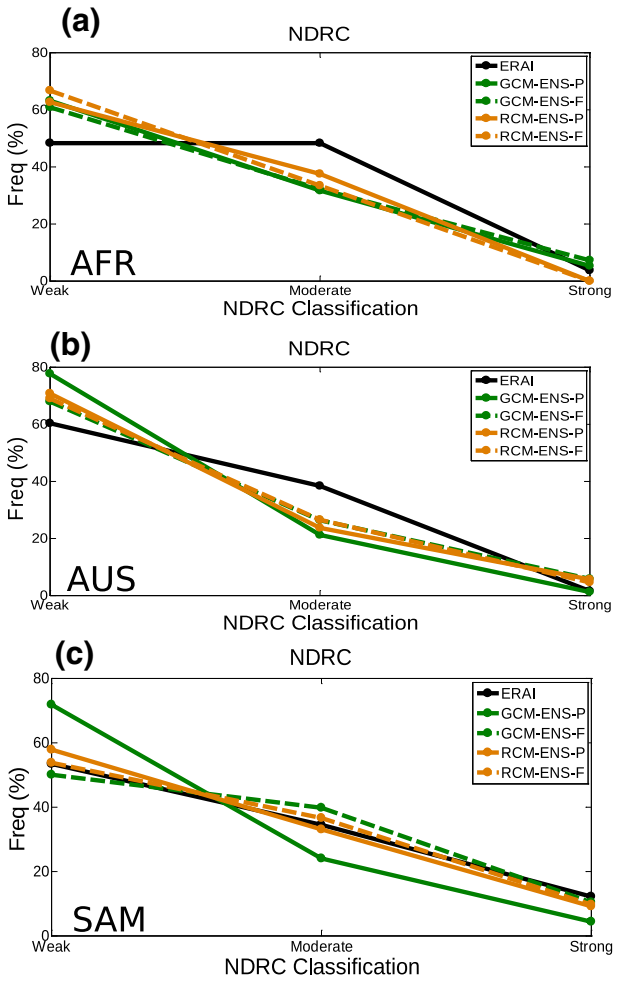

Fig. 5 Frequency polygon of the Normalised Central Pressure Deepening Rate (NDRC) of EECs following Sanders (1986) classification: weak ($1.0 \leq \text{NDR} < 1.3$), moderate ($1.3 \leq \text{NDR} < 1.8$) and strong ($\text{NDR} \geq 1.8$) for **a** AFR, **b** AUS and **c** SAM domains

3.5 EEC composites

3.5.1 Africa

3.5.1.1 Genesis In RegCM4, EECs in AFR show a deeper center in future climate (1001.3 hPa) compared to present (1004.2 hPa) during the cyclogenesis phase (Fig. 6c, d; Table S1). Even though the GCMs ensemble does not indicate a strengthening of the central pressure of EECs as in RegCM4, the curvature of isobars is more pronounced in the future time slice compared to the present (Fig. 6a, b). In addition, the GCMs ensemble projects more precipitation around the center of the cyclone, near the warm front region (Fig. 6a, b) as also found in other studies (e.g. Yettella and Kay 2017; Catto et al. 2019; Sinclair et al. 2020). This pattern is less clear in RegCM4 (Fig. 6c, d), where the precipitation increase is only noted far from the cyclone center in the future. There are some discontinuities in the RegCM4 composites over the southern regions due to the proximity of cyclones to the border.

EGR practically does not change its intensity in the future climate in the GCMs while it is projected to weaken in RegCM4; on the other hand, the cyclonic circulation at 850 hPa in both ensembles is better defined during the genesis phase in the future (Fig. 6e–h). Hence, the projections indicate in the future a large-scale decrease of the environmental baroclinicity in RegCM4. However, this feature does not decrease the wind intensity at low levels in RegCM4 (Figure S1b), suggesting that diabatic processes might play a greater role in the intensification of the cyclonic circulation, as observed in various explosive developments in present climate (e.g. Dias Pinto and da Rocha 2011; Fink et al. 2012; Flaounas et al. 2021). For both ensembles, in the future climate, the maximum EGR occurs with a northwest-southeast orientation, similar to the climatological pattern of all cyclones (e.g. Crespo et al. 2020b), accompanied by stronger winds behind the warm front (Fig. 6e–h).

3.5.1.2 Explosive phase During the explosive phase of EECs, precipitation is projected to be more intense in the future, with a deeper cyclone center in both ensembles (Fig. 7a–d). RegCM4 shows higher amounts of precipitation near the center of the cyclone and the warm front, while the frontal structure is not evident in the rainfall simulated by the GCMs because of their coarse resolution (Fig. 7a–d). The RegCM4 composites in Fig. 7 show a larger region of discontinuity south of the center compared to the genesis phase (Fig. 6c, d) due to the fast motion of EECs to the southeast, reaching latitudes close to the boundary (Fig. 1). It is interesting to note that the GCMs ensemble projects a larger and more elongated north–south low-pressure system (Fig. 7a, b), which also occurs in the genesis phase (Fig. 6a, b). This difference in structure reflects the trough predominance in GCMs due to the stronger westerly winds, while the cyclonic circulation is better defined in RegCM4 (Fig. 7e, f). In the present climate, two distinct maxima of EGR are simulated clearly in the GCMs (Fig. 7e) surrounding the cyclones. In RegCM4, the EGR field is noisier in the southern part of the cyclone region but the EGR surrounds the cyclones in both periods (Fig. 7g, h). Despite the difference in spatial EGR pattern within the GCMs and RegCM4 ensembles, both project a weakening in the future compared to the present (Fig. 7f), which implies a less baroclinic environment. Therefore, the projections of deeper EECs in the future indicate an increase of the contribution of diabatic heating (more details in Sect. 3.5.4).

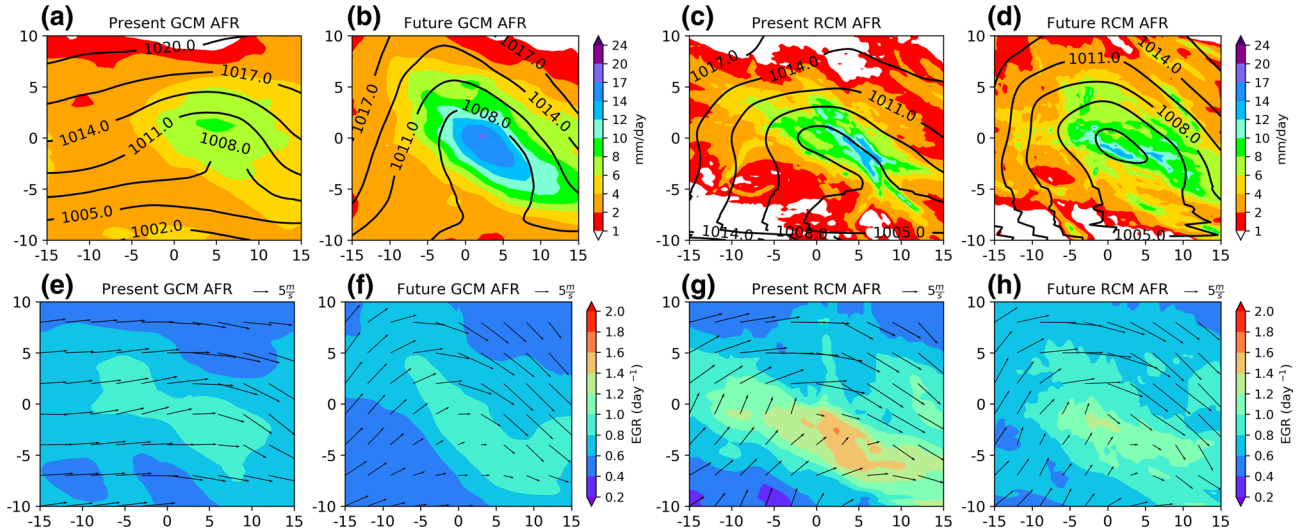

Fig. 6 Composites of **a**–**d** precipitation (shaded; mm day^{-1}) and MSLP (black lines; hPa); **e**–**h** EGR in the layer 850–500 hPa (shaded; day^{-1}) and wind vectors at 850 hPa (m s^{-1}) in present and future climates in **a**, **b**, **e**, **f** GCMs and **c**, **d**, **g**, **h** RegCM4 during EECs genesis occurring in the Africa domain. All composites are centered in the cyclone center (0) and the axes indicate degrees east (positive)/west (negative) and north (positive)/south (negative)

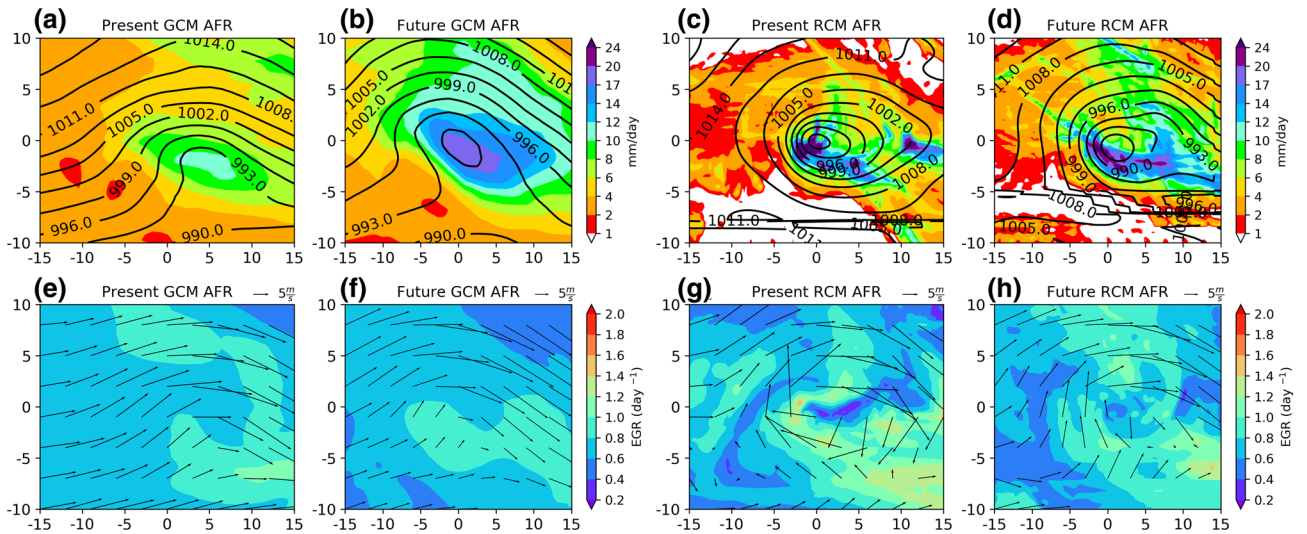

Fig. 7 Similar to Fig. 6 but for the explosive phase of EECs occurring in the Africa domain

3.5.2 Australia

3.5.2.1 Genesis For the AUS domain, EECs are deeper (Fig. 8a–d) compared to AFR (Fig. 6a–d). During the genesis phase, only the GCMs ensemble projects stronger EECs in the future climate (990.2 hPa) compared to the present (994.4 hPa), while RegCM4 indicates similar intensities (994 hPa) in both periods (Fig. 8a, b; Table S1). For both ensembles and time slices, EGR shows a similar structure (Fig. 8e, f), however, the EGR from RegCM4 is consistently higher than in the GCMs in the present climate. The projections for low-level circulation indicate, in general, stronger (weaker) winds in the northern and eastern (southern) sectors of the cyclones (i.e., ahead of the cold front or behind the warm front) in future climate conditions in both ensembles (Figure S2a-b). RegCM4 projections for the future are in line with the reanalysis trends that indicate a decrease in the growth rate near the Australian coast (Osbrough and Frederiksen 2021). The ensembles project higher amounts of precipitation in the future, similar to the projections of pre-

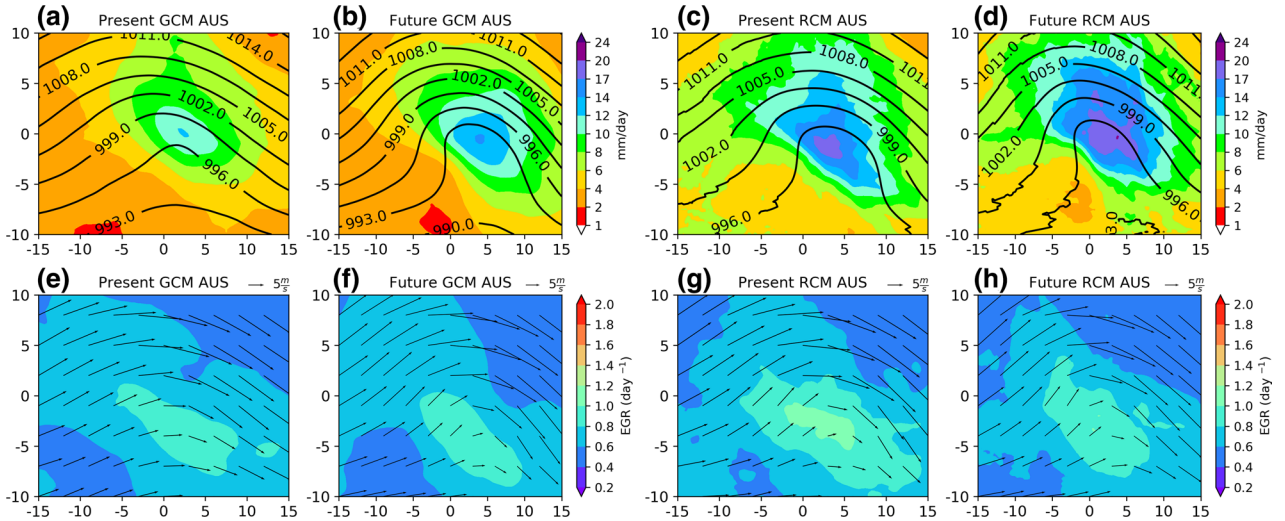

Fig. 8 Composites of **a**–**d** precipitation (shaded; mm day^{-1}) and MSLP (black lines; hPa); **e**–**h** EGR in the layer 850–500 hPa (shaded; day^{-1}) and wind vectors at 850 hPa (m s^{-1}) in present and future climates in **a**, **b**, **e**, **f** GCMs and **c**, **d**, **g**, **h**) RegCM4 during EECs genesis occurring in the Australia domain. All composites are centered in the cyclone center (0) and the axes indicate degrees east (positive)/west (negative) and north (positive)/south (negative)

cipitation for all extratropical cyclones in the SH (Reboita et al. 2020). Furthermore, RegCM4 simulates more intense precipitation occupying a larger area north of the cyclone center than the GCMs (Fig. 8a–d).

3.5.2.2 Explosive phase EECs in AUS are projected to be deeper in the GCMs (~5 hPa) and RegCM4 (~2 hPa) in the future climate during the explosive phase (Fig. 9a–d; Table S1). According to the GCMs projections, the difference of precipitation between present and future climate is quite small (Fig. 9a–b). On the other hand, RegCM4 projects a stronger intensification of precipitation in the future climate, especially near the center of the cyclone and along the warm front (Fig. 9c, d). In terms of baroclinicity, the northwest-southeast oriented band of EGR in both time slices are similar, however, with lower values in the future for both ensembles (Fig. 9e–h). The maximum values of EGR are found in the southern sector of the cyclones, to the south of the most intense precipitation region during the explosive phase. The explosive phase of EECs is thus pro-

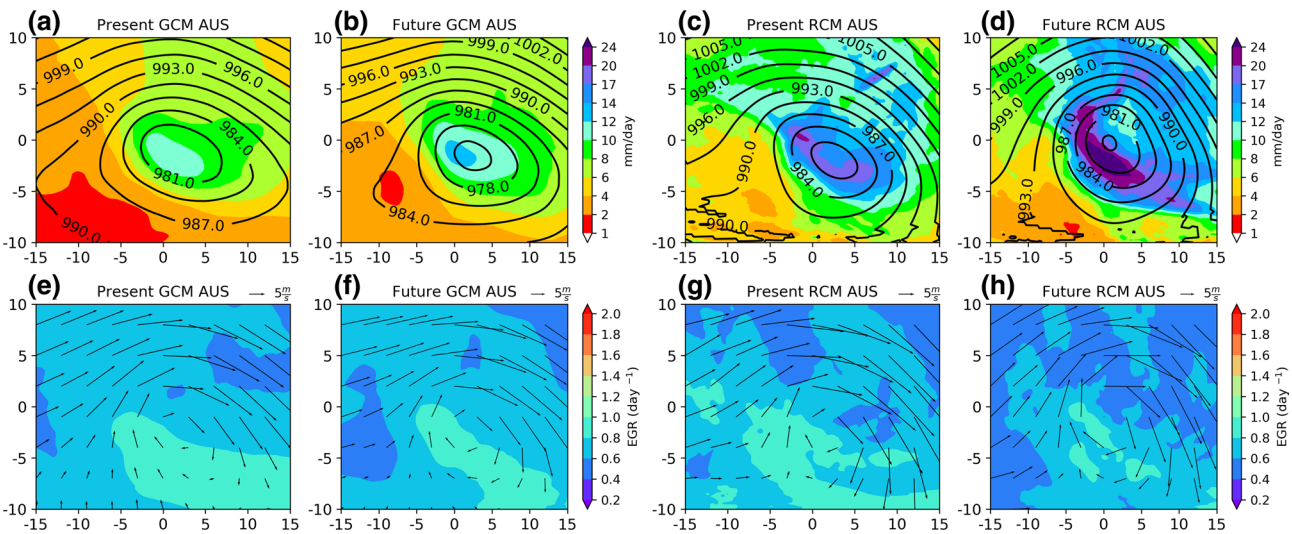

Fig. 9 Similar to Fig. 8 but for the explosive phase of EECs occurring in the Australia domain

jected to occur in a large-scale less baroclinic environment, having stronger precipitation around the cyclone centers and achieving lower central pressures. For the future, both ensembles also indicate an intensification of the circulation at 850 hPa in center-north sectors of the cyclone (Figure S2c-d).

3.5.3 South America

3.5.3.1 Genesis EECs in the SAM domain are weaker than in AUS but, in general, stronger than in AFR during genesis (Table S1), and are better configured (closed isobar) in RegCM4 than in the GCMs (Fig. 10a ,c). For the future, the GCMs project deeper EECs (~2 hPa), slightly stronger low-level winds at the north sector of the EECs and an intensification of the precipitation near the center of the cyclone. RegCM4 projections are similar to the GCMs, but with the variables showing lower intensity than the global models (Fig. 10b, d). EGR has a similar spatial configuration in RegCM4 and the GCMs, however, RegCM4 presents higher values of EGR than the GCMs in both time slices. On the other hand, the GCMs ensemble projects higher EGR values in the future climate compared to present, which is not the case for RegCM4 (Fig. 10e–h). Hence, only the GCMs project a slightly more baroclinic environment during the genesis of EECs in the future.

3.5.3.2 Explosive phase During the explosive phase, EECs in SAM are very similar to the AUS EECs in terms of strength and structure and also present an intensification of precipitation in the future. The structure of EGR in SAM resembles the ones from AUS, with both ensembles projecting weaker EGR in the future climate (Fig. 11e–h) in agreement with previous studies (Caballero and Langen 2005; Seiler and Zwiers 2016a; Seiler et al. 2018). In terms of low-level circulation, the GCMs project an intensification of the winds at the same places where precipitation is projected to increase, while RegCM4 indicates slightly weaker winds (Figure S3d). We suggest that the intensification of precipitation, which is associated with diabatic heating, is contributing to deeper cyclones in the GCMs and, consequently, stronger winds in the future.

3.5.4 Discussion

In all domains, the EGR does not show large differences between the future and present climates during the cyclogenesis phase but, in general, it is weaker during the explosive phase of the EECs in the future climate. Osbrough and Frederiksen (2021), based on a review of the literature, mention that CMIP3 and CMIP5 projections from skilful GCMs also indicate future decreases in baroclinicity over the latitude belt around 30° S, with increases near 55° S for high CO_2 emission scenarios.

In both the genesis and explosive phases, the EECs are projected to become mostly deeper and with more intense precipitation (mainly in the warm front sector) in the future climate. These results are in line with studies showing that the moisture content in the atmosphere is increased in a

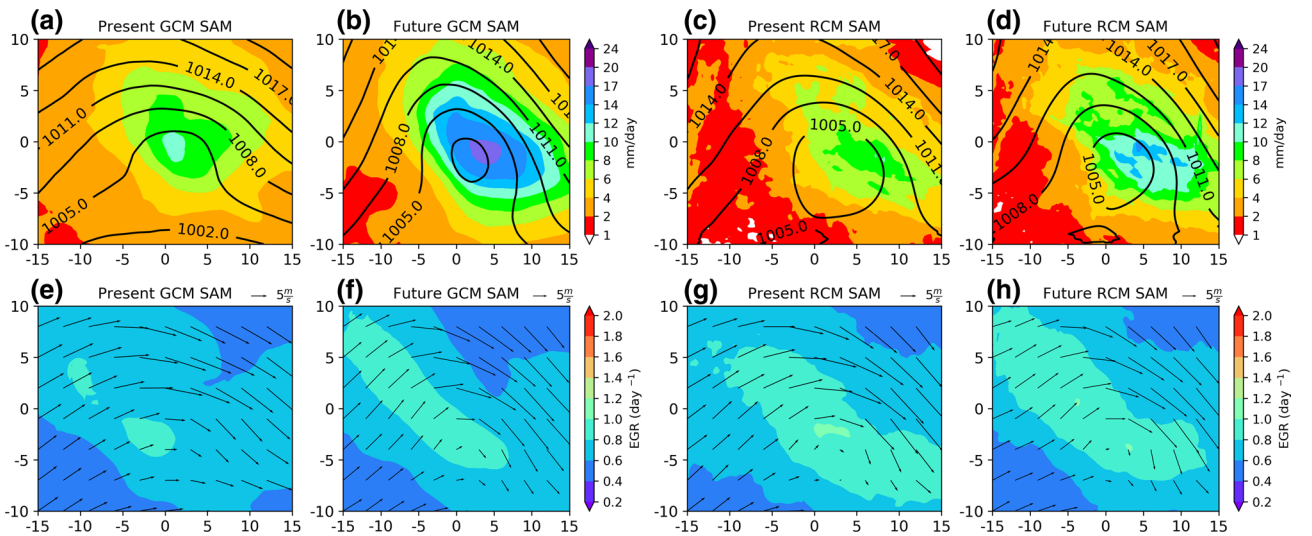

Fig. 10 Composites of **a**–**d** precipitation (shaded; mm day^{-1}) and MSLP (black lines; hPa); **e**–**h** EGR in the layer 850–500 hPa (shaded; day^{-1}) and wind vectors at 850 hPa (m s^{-1}) in present and future climates in **a**, **b**, **e**, **f** GCMs and **c**, **d**, **g**, **h** RegCM4 during EECs genesis occurring in the South America domain. All composites are centered in the cyclone center (0) and the axes indicate degrees east (positive)/west (negative) and north (positive)/south (negative)

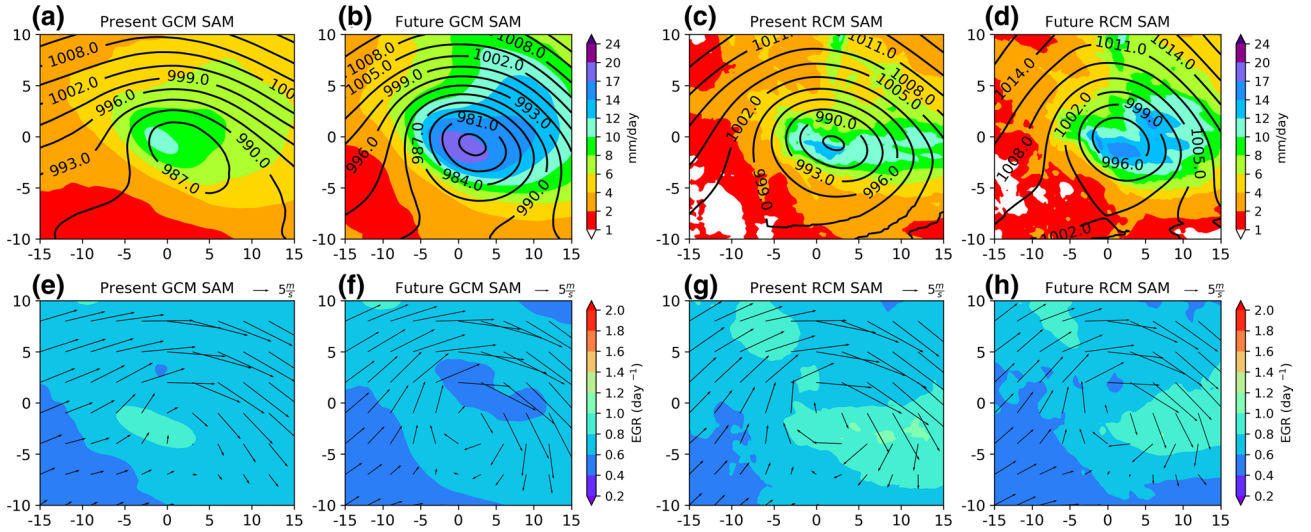

Fig. 11 Similar to Fig. 10 but for the explosive phase of EECs occurring in the South America domain

warmer climate (Yettella and Kay 2017; Catto et al. 2019; Gertler and O'Gorman 2019; Sinclair et al. 2020) but, at the same time, wetter conditions help to decrease the intensity of the meridional temperature gradients at low and mid-levels of the atmosphere (Gertler and O'Gorman 2019) being a negative effect for extratropical cyclones. As discussed by Caballero and Lagen (2005) and Hwang and Frierson (2010), the decrease of baroclinicity is related to the fact that the increase in air temperature enhances the poleward latent heat transport, and the condensation helps to warm the atmosphere at high latitudes (although latent heat transport increases with the increase of temperature, it does not do so indefinitely; when the meridional temperature gradient weakens, the latent heat transport tends to stabilize). Caballero and Lagen (2005) also propose that other processes, such as the melting of ice and snow cover through surface albedo feedbacks, can contribute to weakening the meridional temperature gradient. As the horizontal temperature gradients are a lifting mechanism, the upward air movement is weakened and, as a consequence, the static stability is increased (Frierson 2006; Frierson et al. 2006), leading to a decrease in EGR (Caballero and Langen 2005). Therefore, the cyclones become less baroclinic (which is shown by the low values of EGR in the future) in terms of large scale conditions.

The reason for EECs to become deeper and with intensified precipitation in the future might be associated with the future wetter environment, which contributes to intensify diabatic processes (latent heat release associated with condensation). A proxy of these processes is the projected increase of precipitation along the warm front contributing to warming the warm sector of the extratropical cyclones, with the consequent strengthening of the local baroclinicity, resulting in deeper EECs. This physical explanation is summarized in Fig. 12. The increase of precipitation produced by EECs and other categories of extratropical cyclones (Reboita et al. 2020) also helps to explain the increase in the precipitation towards the south pole in future climate projected by IPCC models (IPCC 2013).

4 Conclusions

EECs are synoptic-scale systems, which experience a fast deepening rate over a relatively short time range (~ 24 hPa/24 h), and are often associated with severe weather (Sanders and Gyakum 1980). We investigated future changes in EECs during austral winter in GCMs and RegCM4 ensemble projections for three SH domains (AFR, SAM and AUS) under the RCP8.5 scenario. The main results can be summarized as follows:

- EECs represent ~ 13–17% of the total number of extratropical cyclones in the ERAI reanalysis during the austral winter. The ensembles underestimate this proportion. While in the AFR domain the GCMs ensemble has a percentage of EECs closer to ERAI, in the AUS and SAM domains the RegCM4 ensemble is closer to the reanalysis;
- RegCM4 ensemble projects an increase of 19% for SAM and 33% for AFR in the frequency of EECs, while no relevant changes are projected in AUS. Although the signs of the change of EECs are consistent with those already discussed in the scientific literature (Chang et al. 2012; Seil et al. 2018) their magnitudes need to be considered with caution because they are smaller than the underesti-

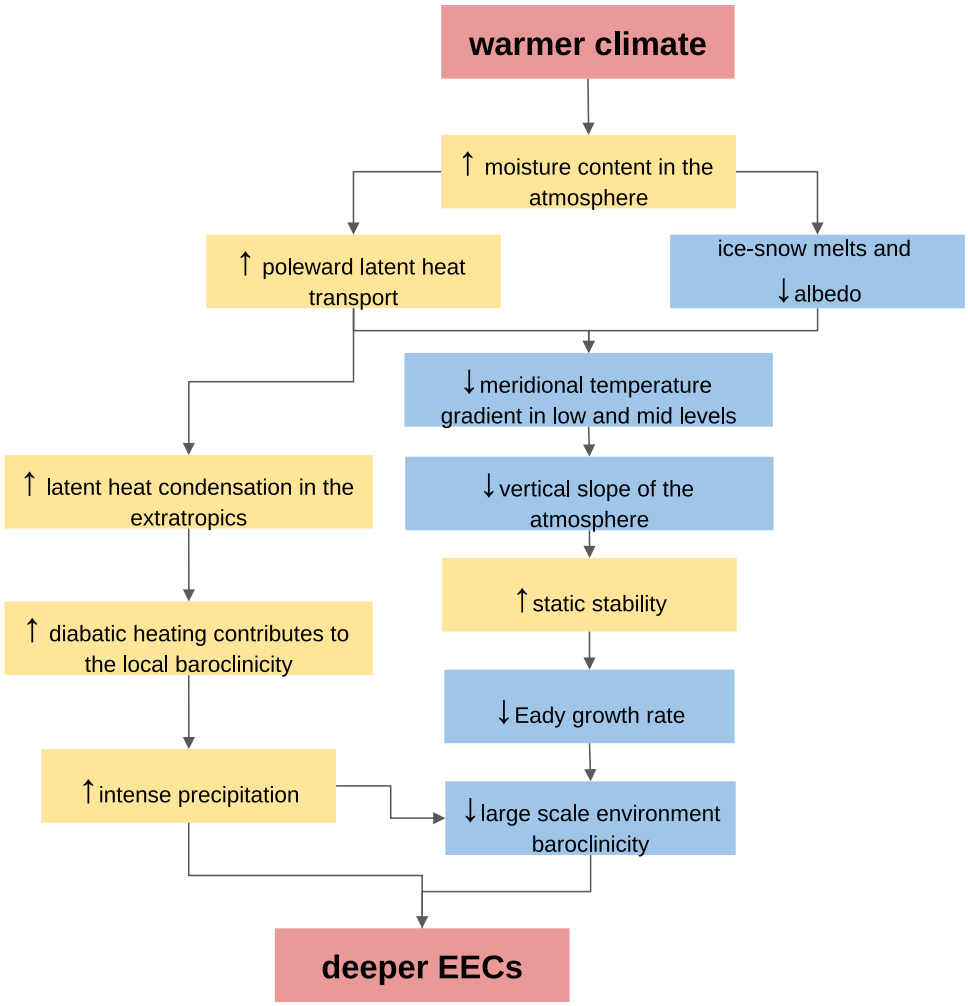

Fig. 12 Diagram of the physical processes associated with the changes projected for EECs (vide text for more details); ↑ = increase, ↓ = decrease

mation in the frequency of EECs in the RegCM4 ensemble in the present climate;

- the proportion of EECs compared to the total number of extratropical cyclones (EECs/total) in each domain during the austral winter is projected to increase in the future period compared to the present, with higher positive changes for the SAM domain (7.4% in GCMs and 5.6% in RegCM4) than AFR (3.3% in GCMs and 3.9% in RegCM4) and AUS (3.9% in GCMs and 1.7% in RegCM4);
- although the frequency of EECs is projected to increase in the future climate, it does not show a positive linear trend due to the large interannual/interdecadal variability;
- EECs in the future will be deeper and faster but with a shorter lifetime compared to the present climate, and
- composites show that in the genesis and explosive phases over all subdomains, EECs tend to become deeper and with more intense precipitation in future warmer conditions, mainly along the cyclone center and the warm front. On the other hand, as indicated by the EGR changes, the large-scale baroclinicity is projected to decrease, and this implies that the diabatic heating acts to strengthen the local baroclinicity in the EECs. This process explains the deeper cyclones, the intensification of EEC rainfall and stronger low-level winds in the warm sector of the EECs in the future climate. A simple illustration in Fig. 13 summarizes these main findings.

In brief, our results project for the future an increase of the frequency of EECs, with consequent changes in low-level winds and precipitation in the SH. In terms of physical mechanisms, we find an increase in the thermodynamic contribution to the EEC development and a decrease in the dynamic ones. These results are for austral winter. Although EECs are less frequent in the other seasons, it would be important to investigate if these changes are projected throughout the year. As discussed, the Sanders and Gyakum (1980) formulation to identify EECs may not include cyclones that deepen rapidly over periods of less than 24 h. Therefore, in a next investigation it would be very important to evaluate the sensitivity of the EECs

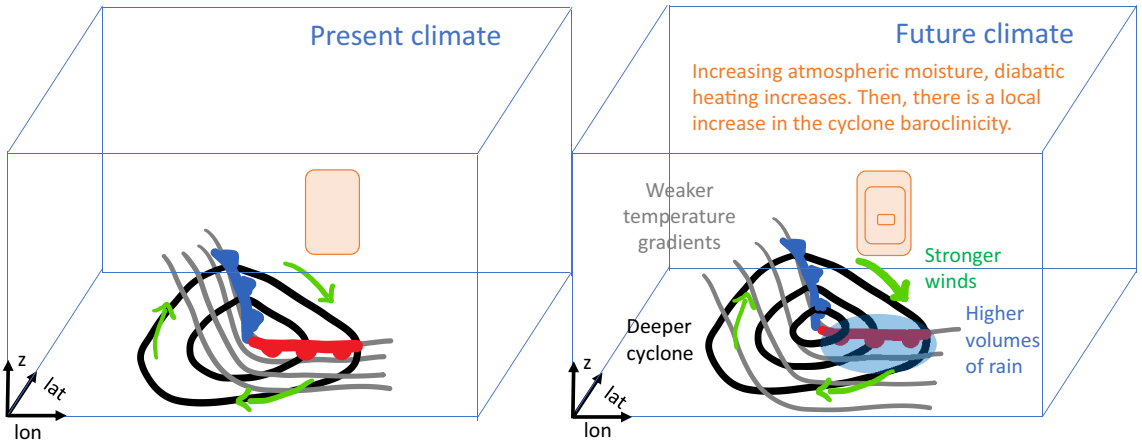

Fig. 13 Schematic illustration showing the main features of EECs in present (left side) and future (right side) climates in the SH

climatology and climate change signal as a function of the detection criterion used.

Supplementary Information The online version contains supplementary material available at https://doi.org/10.1007/s00382-021-05867-w.

Acknowledgements We thank the international centers that provided data for this study. We also thank Conselho Nacional de Desenvolvimento Científico e Tecnológico (CNPq) and PETROBRAS from Brazil for the financial support. M.Reale has been supported in this work by OGS and CINECA under HPC-TRES award number 2015-07 and by the project FAIRSEA (Fisheries in the Adriatic Region - a Shared Ecosystem. Approach) funded by the 2014 - 2020 Interreg V-A Italy - Croatia CBC Programme (Standard project ID 10046951).

Data Availability The authors declare that all data used in this study are freely available in online repositories described in the methodology.

References

Allen JT, Pezza AB, Black T (2010) Explosive cyclogenesis: a global climatology comparing multiple reanalyses. J Clim 23:6468–6484. https://doi.org/10.1175/2010JCLI3437.1

Ambrizzi T, Reboita MS, da Rocha RP, Llopart M (2019) The state of the art and fundamental aspects of regional climate modeling in South America. Ann N Y Acad Sci 1436:98–120. https://doi.org/10.1111/nyas.13932

Bader J, Mesquita MD, Hodges KI, Keenlyside N, Østerhus S, Miles M (2011) A review on Northern Hemisphere sea-ice, storminess and the North Atlantic Oscillation: observations and projected changes. Atmos Res 101:809–834. https://doi.org/10.1016/j.atmosres.2011.04.007

Bentsen M, Bethke I, Debernard JB, Iversen T, Kirkevåg A, Seland Ø, Dranges H, Roelandt C, Seierstad IA, Hoose C, Kristj´ansson JE (2013) The Norwegian earth system model, NorESM1-M—Part 1: description and basic evaluation of the physical climate. Geosci Model Dev 6:687–720. https://doi.org/10.5194/gmd-6-687-2013

Bitencourt DP, Fuentes MV, Cardoso CDS (2013) Climatologia de ciclones explosivos para a área ciclogenética da América do Sul. Rev Bras Meteorol 28:43–56. https://doi.org/10.1590/S0102-77862013000100005

Bjerknes J, Solberg H (1922) Life cycle of cyclones and the Polar Front theory of atmospheric circulation. Geophys Publik 3:3–18

Black MT, Pezza AB, Kreft P (2010) An examination of Southwest Pacific explosive cyclones, 1989 to 2009. IOP Conf Ser: Earth Environ Sci 11:012036. https://doi.org/10.1088/1755-1315/11/1/012036

Bullock TA, Gyakum JR (1993) A diagnostic study of cyclogenesis in the western North Pacific Ocean. Mon Wea Rev 121:65–75. https://doi.org/10.1175/1520-0493(1993)121%3c0065:ADSOCI%3e2.0.CO;2

Caballero R, Langen PL (2005) The dynamic range of poleward energy transport in an atmospheric general circulation model. Geophys Res Lett 32:L02705. https://doi.org/10.1029/2004GL021581

Carlson TN (1991) Mid-latitude weather systems. Harper Collins, London, p 512

Catto JL, Ackerley D, Booth JF, Champion AJ, Colle BA, Pfahl S, Pinto JG, Quinting JF, Seiler C (2019) The future of midlatitude cyclones. Curr Clim Change Rep 5(407):420. https://doi.org/10.1007/s40641-019-00149-4

Chang EKM (2017) Projected Significant Increase in the Number of Extreme Extratropical Cyclones in the Southern Hemisphere. J Clim 30:4915–4935

Chang EK, Guo Y, Xia X (2012) CMIP5 multimodel ensemble projection of storm track change under global warming. J Geophys Res 117:D23118. https://doi.org/10.1029/2012JD018578

Chen SJ, Kuo YH, Zhang PZ, Bai QF (1992) Climatology of explosive cyclones off the East Asian coast. Mon Wea Rev 120:3029–3035. https://doi.org/10.1175/1520-0493(1992)120%3c3029:COECOT%3e2.0.CO;2

Chen GTJ, Lu CF (1997) On the climatological aspects of explosive cyclones over the Western North Pacific and East Asia Coastal areas. Terr Atmos Ocean Sci 8:427–442

Cione JJ, Raman S (1995) A numerical investigation of surface-induced mesocyclogenesis near the Gulf Stream. Tellus A 47:815–833. https://doi.org/10.1034/j.1600-0870.1995.00122.x

Cohen J (2011) Explosive cyclones. In: Schneider SH, Root TL, Mastrandrea MD (eds) Encyclopedia of climate and weather, volume 1. Oxford University Press, pp. 339–344

Collins WJ, Bellouin N, Doutriaux-Boucher M, Gedney N, Hinton T, Jones CD, Liddicoat S, Martin G, O'Connor F, Rae J, Senior C, Totterdell I, Woodward S, Reichler T, Kim J, Halloran P (2008) Evaluation of the HadGEM2 model. Hadley Centre Technical

Note HCTN 74, Met Office Hadley Centre, Exeter, UK. https://www.metofce.gov.uk/learning/library/publications/science/climate-science

Crescenti GH, Weller RA (1992) Analysis of surface fluxes in the marine atmospheric boundary layer in the vicinity of rapidly intensifying cyclones. J Appl Meteorol 31:831–848. https://doi.org/10.1175/1520-0450(1992)031%3c0831:AOSFIT%3e2.0.CO;2

Crespo NM, da Rocha RP, De Jesus EM (2020a) Cyclones density and characteristics in different reanalyses dataset over South America. In: EGU general assembly 2020. https://doi.org/10.5194/egusphere-egu2020-11316. Online, 4–8 May 2020, EGU2020-11316

Crespo NM, da Rocha RP, Sprenger M, Wernli H (2020b) A potential vorticity perspective on cyclogenesis over centre-eastern South America. Int J Climatol 2020:1–16. https://doi.org/10.1002/joc.6644

Danard MB, Ellenton GE (1980) Physical influences on East Coast cyclogenesis. Atmos Ocean 18(1):65–82

Davis CA (2018) Resolving tropical cyclone intensity in models. Geophys Res Lett 45(4):2082–2087. https://doi.org/10.1002/2017GL076966

Dee DP, Uppala SM, Simmons AJ, Berrisford P, Poli P, Kobayashi S, Andrae U, Balmaseda MA, Balsamo G, Bauer P, Bechtold P, Beljaars ACM, van de Berg L, Bidlot J, Bormann N, Delson C, Dragani R, Fuentes M, Geer AJ, Haimberger L, Healy SB, Hersbach H, Hólm EV, Isaksen L, Kallberg P, Kohler M, Matricardi M, McNally AP, Monge-Sanz BM, Morcrette JJ, Park BK, Peubey C, Rosnay P, Tavolatto C, Thépaut JN, Vitart F (2011) The ERA-Interim reanalysis: configuration and performance of the data assimilation system. Q J Roy Meteorol Soc 137:553–597. https://doi.org/10.1002/qj.828

Dias Pinto JR, da Rocha RP (2011) The energy cycle and structural evolution of cyclones over southeastern South America in three case studies. J Geophys Res Atmos. https://doi.org/10.1029/2011JD016217

Eiras-Barca J, Ramos AM, Pinto JG, Trigo RM, Liberato ML, Miguez-Macho G (2018) The concurrence of atmospheric rivers and explosive cyclogenesis in the North Atlantic and North Pacific basins. Earth Syst Dynam 9:91. https://doi.org/10.5194/esd-9-91-2018

Fink AH, Pohle S, Pinto JG, Knippertz P (2012) Diagnosing the influence of diabatic processes on the explosive deepening of extratropical cyclones. Geophys Res Lett. https://doi.org/10.1029/2012GL051025

Flaounas E, Gray SL, Teubler F (2021) A process-based anatomy of Mediterranean cyclones: from baroclinic lows to tropical-like systems. Weather Clim Dynam 2:255–279. https://doi.org/10.5194/wcd-2-255-2021

Flaounas E, Kelemen FD, Wernli H, Gaetner MG, Reale M, Sanchez-Gomez E, Lionello P, Calmanti S, Podracanin Z, Somot S, Akhtar N, Romera R, Conte D (2018) Assessment of an ensemble of ocean–atmosphere coupled and uncoupled regional climate models to reproduce the climatology of Mediterranean cyclones. Clim Dyn 51:1023–1040

Frierson DMW (2006) Robust increases in midlatitude static stability in simulations of global warming. Geophys Res Lett 33:L24816. https://doi.org/10.1029/2006GL027504

Frierson DMW, Held IM, Zurita-Gotor P (2006) A gray-radiation aquaplanet moist GCM. Part I: static stability and eddy scale. J Atmos Sci 63:2548–2566. https://doi.org/10.1175/JAS3753.1

Fu G, Sun Y, Sun J, Li P (2020) A 38-year climatology of explosive cyclones over the Northern Hemisphere. Adv Atmos Sci 37:143–159. https://doi.org/10.1007/s00376-019-9106-x

Gan MA, Rao VB (1991) Surface cyclogenesis over South America. Mon Weather Rev 119(5):1293–1302

Gentry MS, Lackmann GM (2010) Sensitivity of simulated tropical cyclone structure and intensity to horizontal resolution. Mon Weather Rev 138:688–704. https://doi.org/10.1175/2009MWR2976.1

Gertler CG, O'Gorman PA (2019) Changing available energy for extratropical cyclones and associated convection in Northern Hemisphere summer. Proc Natl Acad Sci 116(10):4105–4110. https://doi.org/10.1073/pnas.1812312116

Giorgetta MA, Jungclaus J, Reick CH, Legutke S, Bader J, Böttinger M, Brovkin V, Crueger T, Esch M, Fieg K, Glushak K, GaylerV HH, Hollweg H, Ilyina T, Kinne S, Kornblueh L, Matei D, Mauritsen T, Mikolajewicz U, Mueller W, Notz D, Pithan F, Raddatz T, Rast S, Redler R, Roeckner E, Schmidt H, Schnur R, Segschneider J, Six K, Stockhause M, Timmreck C, Wegner J, Widmann H, Wieners K, Claussen M, Marotzke J, Stevens B (2013) Climate and carbon cycle changes from 1850 to 2100 in MPI-ESM simulations for the Coupled Model Intercomparison Project phase 5. J Adv Model Earth Syst 5:572–597

Giorgi F, Coppola E, Solmon F, Mariotti L, Sylla MB, Bi X, Elguindi N, Diro GT, Nair V, Giuliani G, Turuncoglu UU, Cozzini S, Guttler I, Obrien TA, Tawfik AB, Shalaby A, Zakey AS, Steiner AL, Stordal F, Sloan LC, Brankovic C (2012) RegCM4: model description and preliminary tests over multiple COR-DEX domains. Clim Res 52:7–29. https://doi.org/10.3354/cr01018

Giorgi F, Jones C, Asrar GR (2009) Addressing climate information needs at the regional level: the CORDEX Framework. World Meteorol Organ (WMO) Bull 58(3):175

Gramcianinov CB, Campos RM, Soares CG, Camargo R (2020) Extreme waves generated by cyclonic winds in the western portion of the South Atlantic Ocean. Ocean Eng 213:107745

Gutowski WJ Jr, Giorgi F, Timbal B, Frigon A, Jacob D, Kang H-S, Raghavan K, Lee B, Lennard C, Nikulin G, O'Rourke E, Rixen M, Solman S, Stephenson T, Tangang F (2016) WCRP coordinated regional downscaling experiment (CORDEX): a diagnostic MIP for CMIP6. Geosci Model Dev 9:4087–4095. https://doi.org/10.5194/gmd-9-4087-2016

Gyakum JR (1983a) On the evolution of the QE-II storm. I: synoptic aspects. Mon Weather Rev 111:1137–1155. https://doi.org/10.1175/1520-0493(1983)111%3c1137:OTEOTI%3e2.0.CO;2

Gyakum JR (1983b) On the evolution of the QE-II storm. II: dynamic and thermodynamic structure. Mon Weather Rev 111:1156–1173. https://doi.org/10.1175/1520-0493(1983)111%3c1

Heo KY, Ha KJ, Ha T (2019) Explosive Cyclogenesis around the Korean Peninsula in May 2016 from a potential vorticity perspective: case study and numerical simulations. Atmosphere 10:22. https://doi.org/10.3390/atmos10060322

Holton JR (2004) An introduction to dynamic meteorology. Acad Press, Amsterdam

Hoskins BJ, Hodges KI (2005) A new perspective on Southern Hemisphere storm tracks. J Clim 18(20):4108–4129

Hoskins BJ, Valdes PJ (1990) On the existence of storm-tracks. J Atmos Sci 47(15):1854–1864

Hwang Y-T, Frierson DMW (2010) Increasing atmospheric poleward energy transport with global warming. Geophys Res Lett 37:L24807. https://doi.org/10.1029/2010GL045440

IPCC (2013) Climate change 2013: the physical science basis. Contribution of working group I to the fifth assessment report of the intergovernmental panel on climate change. Cambridge University Press, Cambridge and New York, NY 1535. https://doi.org/10.1017/CBO9781107415324

Kodama C, Stevens B, Mauritsen T, Seiki T, Satoh M (2019) A new perspective for future precipitation change from intense extratropical cyclones. Geophys Res Lett 46:12435–12444. https://doi.org/10.1029/2019GL084001

Kouroutzoglou J, Flocas HA, Keay K, Simmonds I, Hatzaki M (2011) Climatological aspects of explosive cyclones in the

Mediterranean. Int J Climatol 31:1785–1802. https://doi.org/10.1002/joc.2203

Kuo YH, Reed RJ (1988) Numerical simulation of an explosively deepening cyclone in the eastern Pacific. Mon Weather Rev 116:2081–2105. https://doi.org/10.1175/1520-0493(1988)116%3c2081:NSOAED%3e2.0.CO;2

Kuwano-Yoshida A, Asuma Y (2008) Numerical study of explosively developing extratropical cyclones in the northwestern Pacific region. Mon Weather Rev 136:712–740. https://doi.org/10.1175/2007MWR2111.1

Kuwano-Yoshida A, Sasaki H, Sasai Y (2016) Impact of explosive cyclones on the deep ocean in the North Pacific using an eddy-resolving ocean general circulation model. Geophys Res Lett. https://doi.org/10.1002/2016GL071367

Leslie LM, Leplastrier M, Buckley BW, Qi L (2005) Climatology of meteorological "bombs" in the New Zealand region. Meteorol Atmos Phys 89:207–214. https://doi.org/10.1007/s00703-005-0129-8

Liberato MLR, Pinto JG, Trigo IF, Trigo RM (2011) Klaus - an exceptional winter storm over northern Iberia and southern France. Weather 66:330–334. https://doi.org/10.1002/wea.755

Lim EP, Simmonds I (2002) Explosive cyclone development in the Southern Hemisphere and a comparison with Northern Hemisphere events. Mon Weather Rev 130:2188–2209. https://doi.org/10.1175/1520-0493(2002)130%3c2188:ECDITS%3e2.0.CO;2

Lionello P, Conte D, Reale M (2019) The effect of cyclones crossing the Mediterranean region on sea level anomalies on the Mediterranean Sea coast. Nat Hazards Earth Syst Sci 19:1541–1564. https://doi.org/10.5194/nhess-19-1541-2019,2019

Lionello P, Dalan F, Elvini E (2002) Cyclones in the Mediterranean region: the present and the doubled CO2 climate scenarios. Clim Res 22:147–159. https://doi.org/10.3354/cr022147

Lionello P, Trigo IF, Gil V, Liberato ML, Nissen KM, Pinto JG et al (2016) Objective climatology of cyclones in the Mediterranean region: a consensus view among methods with different system identification and tracking criteria. Tellus A Dyn Meteorol Oceanogr 68(1):29391

Lionello P, Barriopedro D, Ferrarin C, Nicholls R., Orlic M, Raicich F, Reale M, Umgiesser G, Vousdoukas M, Zanchettin D (2020) Extremes floods of Venice: characteristics, dynamics, past and future evolution. Nat Hazards Earth Syst Sci Discuss. https://doi.org/10.5194/nhess-2020-359

Di Luca A, Evans JP, Pepler A et al (2015) Resolution sensitivity of cyclone climatology over eastern Australia using six reanalysis products. J Clim 28:9530–9549. https://doi.org/10.1175/JCLI-D-14-00645.1

Marrafon VH, Reboita MS, da Rocha RP, Crespo NM (2021) Extratropical cyclones in the Southern Hemisphere: comparison among different reanalyses. Climatol Brazil J 17(28):48–73. https://doi.org/10.5380/abclima.v28i0.74460

McMurdie L, Houze RA (2006) Weather systems. In: Wallace JM, Hobbs PV (eds) Atmospheric sciences—an introductory survey, 2a edn. Academic Press, London, pp 313–373

Michaelis AC, Willison J, Lackmann GM, Robinson WA (2017) Changes in winter North Atlantic extratropical cyclones in high-resolution regional pseudo–global warming simulations. J Clim 30(17):6905–6925

Neiman PJ, Shapiro MA (1993) The life cycle of an extratropical marine cyclone. Part I: frontal cyclone evolution and thermodynamics air-sea interaction. Mon Weather Rev 121:2153–2176. https://doi.org/10.1175/1520-0493(1993)121%3C2153:TLCOAE%3E2.0.CO;2

Nesterov ES (2010) Explosive cyclogenesis in the northeastern Part of the Atlantic Ocean. Russ Meteorol Hydrol 35:680–686. https://doi.org/10.3103/S1068373910100055

Neu U, Akperov MG, Bellenbaum N, Benestad R, Blender R, Caballero R, Cocozza A, Dacre HF, Feng Y, Fraedrich K, Grieger J, Gulev S, Hanley J, Hewson T, Inatsu M, Keay K, Kew SF, Kindem I, Leckebusch GC, Liberato MLR, Lionello P, Mokhov II, Pinto JG, Raible CC, Reale M, Rudeva I, Schuster M, Simmonds I, Sinclair M, Sprenger M, Tilinina ND, Trigo IF, Ulbrich S, Ulbrish U, Wang XL, Wernli H (2013) Imilast: A community effort to intercompare extratropical cyclone detection and tracking algorithms. Bull Am Meteorol Soc 94:529–547. https://doi.org/10.1175/BAMS-D-11-00154.1

Nuss WA, Anthes RA (1987) A numerical investigation of low-level processes in rapid cyclogenesis. Mon Weather Rev 115:2728–2743. https://doi.org/10.1175/1520-0493(1987)115%3c2728:ANIOLL%3e2.0.CO;2

Osbrough SL, Frederiksen JS (2021) Interdecadal changes in Southern Hemisphere winter explosive storms and Southern Australian rainfall. Clim Dyn. https://doi.org/10.1007/s00382-021-05633-y

Pepler AS, Alexander LV, Evans JP, Sherwood SC (2017) The influence of topography on midlatitude cyclones on Australia's east coast. J Geophys Res Atmos. https://doi.org/10.1002/2017JD027345

Pezza AB, Rashid HA, Simmonds I (2012) Climate links and recent extremes in Antarctic sea ice, high-latitude cyclones, southern annular mode and ENSO. Clim Dyn 38:57–73

Piva DE, Gan MA, de Lima Moscati MC (2011) The role of latent and sensible heat fluxes in an explosive cyclogenesis over the South American East Coast. J Meteor Soci of Japan Ser II 89:637–663. https://doi.org/10.2151/jmsj.2011-604

Reale M, Liberato MLR, Lionello P, Pinto JG, Salon S, Ulbrich S (2019) A global climatology of explosive cyclones using a multi-tracking approach. Tellus 71:1611340. https://doi.org/10.1080/16000870.2019.1611340

Reale M, Lionello P (2013) Synoptic climatology of winter intense precipitation events along the Mediterranean coasts. Nat Hazards Earth Syst Sci 13:1707–1722. https://doi.org/10.5194/nhess-13-1707-2013,2013

Reale M, Cabos W, Cavicchia L, Conte D, Coppola E, Flaounas E, Giorgi F, Hochman A, Li L, Lionello P, Podrascanin Z, Sanchez Gomez E, Scoccimarro E, Sein D, Somot S (2021) Future projections of Mediterranean cyclone characteristics using the Med-CORDEX ensemble of coupled regional climate system models. Clim Dyn, submitted

Reboita MS, Reale M, da Rocha RP, Giorgi F, Giuliani G, Coppola E, Nino RBL, Llopart M, Torres JA, Cavazos T (2020) Future changes in the wintertime cyclonic activity over the CORDEX-CORE southern hemisphere domains in a multi-model approach. Clim Dyn. https://doi.org/10.1007/s00382-020-05317-z

Reboita MS, da Rocha RP, Ambrizzi T (2012) Dynamic and climatological features of cyclonic developments over southwestern South Atlantic Ocean. Horizons Earth Sci Res 6:135–160

Reboita MS, da Rocha RP, Ambrizzi T, Gouveia CD (2015) Trend and teleconnection patterns in the climatology of extratropical cyclones over the southern hemisphere. Clim Dyn 45:1929–1944. https://doi.org/10.1007/s00382-014-2447-3

Reboita MS, da Rocha RP, Ambrizzi T, Sugahara S (2010) South Atlantic Ocean cyclogenesis climatology simulated by regional climate model (RegCM3). Clim Dyn 35(7):1331–1347. https://doi.org/10.1007/s00382-009-0668-7

Reboita MS, da Rocha RP, de Souza MR, Llopart M (2018) Extratropical cyclones over the southwestern South Atlantic Ocean: HadGEM2-ES and RegCM4 projections. Int J Climatol 38(6):2866–2879. https://doi.org/10.1002/joc.5468

Reis PA, Aquino FE, Schossler V, Bernardo RT (2020) Tropical–Antarctic connections of an explosive cyclone in southern Brazil:

rainfall stable isotope ratios and atmospheric analysis. Adv Polar Sci 31:103–111. https://doi.org/10.13679/j.advps.2019.0039
Revell MJ, Ridley RN (1995) The origin and evolution of low-level potential vorticity anomalies during a case of Tasman sea cyclogenesis. Tellus A 47:779–796. https://doi.org/10.1034/j.1600-0870.1995.00120.x
Roebber PJ (1984) Statistical analysis and updated climatology of explosive cyclones. Mon Wea Rev 112(8):1577–1589
Rogers E, Bosart LF (1991) A diagnostic study of two intense oceanic cyclones. Mon Weather Rev 119:965–996. https://doi.org/10.1175/1520-0493(1991)119%3C0965:ADSOTI%3E2.0.CO;2
Sanchez-Gomez E, Somot S (2018) Impact of the internal variability on the cyclone tracks simulated by a regional climate model over the Med-CORDEX domain. Clim Dyn 51(3):1005–1021. https://doi.org/10.1007/s00382-016-3394-y
Sanders F (1986) Explosive Cyclogenesis over the West-Central North Atlantic Ocean, 1981–84. Part II. Evaluation of LFM Model Performance. Mon Wea Rev 114:2207–2218. https://doi.org/10.1175/1520-0493(1986)114%3C2207:ECOTWC%3E2.0.CO;2
Sanders F, Gyakum JR (1980) Synoptic-dynamic climatology of the bomb. Mon Weather Rev 108:1589–1606. https://doi.org/10.1175/1520-0493(1980)108%3C1589:SDCOT%3E2.0.CO;2
Schartner T, Kirchner I (2016) Eady growth rate. Available in https://freva.met.fu-berlin.de/about/eady/
Schossler V, Aquino FE, Reis A, Simões JC (2020) Antarctic atmospheric circulation anomalies and explosive cyclogenesis in the spring of 2016. Theoret Appl Climatol 141:537–549. https://doi.org/10.1007/s00704-020-03200-9
Seiler C, Zwiers FW (2016a) How well do CMIP5 climate models reproduce explosive cyclones in the extratropics of the Northern Hemisphere? Clim Dyn 46:1241–1256. https://doi.org/10.1007/s00382-015-2642-x
Seiler C, Zwiers FW (2016b) How will climate change affect explosive cyclones in the extratropics of the Northern Hemisphere? Clim Dyn 46:3633–3644. https://doi.org/10.1007/s00382-015-2791-y
Seiler C, Zwiers FW, Hodges KI, Scinocca J (2018) How does dynamical downscaling affect model biases and future projections of explosive extratropical cyclones along NorthAmerica's Atlantic coast? Clim Dyn 50:677–692. https://doi.org/10.1007/s00382-017-3634-9
Seluchi ME (1995) Diagnóstico y pronóstico de situaciones sinópticas conducentes a ciclogénesis sobre el este de Sudamérica. Geofísica Internacional 34(2):171–186
Shapiro MA, Keyser D (1990) Fronts, jet streams and the tropopause. In: Newton CW, Holopainen EO (eds.) Extratropical cyclones, the Erik Palmén memorial volume. American Meteorological Society, pp. 167–191
Sinclair MR (1995) An extended climatology of extratropical cyclones over the southern hemisphere. Weather Clim 15:21–32. https://doi.org/10.2307/44279877
Sinclair VA, Rantanen M, Haapanala P, Räisänen J, Järvinen H (2020) The characteristics and structure of extra-tropical cyclones in a warmer climate. Weather Clim Dyn 1:1–25. https://doi.org/10.5194/wcd-1-1-2020
Suzuki-Parker A (2012) Uncertainties and limitations in simulating tropical cyclones. Springer Science & Business Media, New York
Teichmann C, Jacob D, Remedio AR, Remke T, Buntemeyer L, Hoffmann P et al (2021) Assessing mean climate change signals in the global CORDEX-CORE ensemble. Clim Dyn. https://doi.org/10.1007/S00382-020-05494-x
Tonkin H, Holland GJ, Holbrook N, Henderson-Sellers A (2000) An evaluation of thermodynamic estimates of climatological maximum potential tropical cyclone intensity. Mon Weather Rev 128(3):746–762. https://doi.org/10.1175/1520-0493(2000)128%3c0746:AEOTEO%3e2.0.CO;2
Uccellini L, Kocin PJ (1987) The interaction of jet streak circulations during heavy snow events along the east coast of the United States. Weather Forecast 2:289–308
Uccellini LW (1990) Processes contributing to the rapid development of extratropical cyclones. In: Meteorological A (ed) Extratropical cyclones. Society, Boston, pp 81–105
Ulbrich U, Leckebusch GC, Grieger J, Schuster M, Akperov M, Bardin MY et al (2013) Are greenhouse gas signals of Northern Hemisphere winter extra-tropical cyclone activity dependent on the identification and tracking algorithm? Meteorol Z 22(1):61–68
Vera CS, Vigliarolo PK, Berbery EH (2002) Cold season synoptic-scale waves over subtropical South America. Mon Weather Rev 130(3):684–699. https://doi.org/10.1175/1520-0493(2002)130%3c0684:CSSSWO%3e2.0.CO;2
Wang C, Liang J, Hodges KI (2017) Projections of tropical cyclones affecting Vietnam under climate change: downscaled HadGEM2-ES using PRECIS 21. Q J R Meteorol Soc 143(705):1844–1859. https://doi.org/10.1002/qj.3046
Wash CH, Halo RA, Dobos PH, Wright EJ (1992) Study of explosive and nonexplosive cyclogenesis during FGGE. Mon Weather Rev 120:40–51. https://doi.org/10.1175/1520-0493(1992)120%3C0040:SOEANC%3E2.0.CO;2
Willison J, Robinson WA, Lackmann GM (2013) The importance of resolving mesoscale latent heating in the North Atlantic storm track. J Atmos Sci 70:2234–2250. https://doi.org/10.1175/JAS-D-12-0226.1
Yettella V, Kay JE (2017) How will precipitation change in extratropical cyclones as the planet warms? Insights from a large initial condition climate model ensemble. Clim Dyn 49:1765–1781. https://doi.org/10.1007/s00382-016-3410-2
Yoshida A, Asuma Y (2004) Structures and environment of explosively developing extratropical cyclones in the northwestern Pacific region. Mon Wea Rev 132(5):1121–1142
Zhang SQ, Fu G, Lu CG, Liu JW (2017) Characteristics of explosive cyclones over the Northern Pacific. J Appl Meteorol Climatol 56:3187–3210. https://doi.org/10.1175/JAMC-D-16-0330.1
Zhang DL, Radeva E, Gyakum J (1999) A family of frontal cyclones over the western Atlantic Ocean. Part II: parameter studies. Mon Weather Rev 127:1745–1760. https://doi.org/10.1175/1520-0493(1999)127%3C1745:AFOFCO%3E2.0.CO;2

Terms and Conditions

Springer Nature journal content, brought to you courtesy of Springer Nature Customer Service Center GmbH (“Springer Nature”).
Springer Nature supports a reasonable amount of sharing of research papers by authors, subscribers and authorised users (“Users”), for small-scale personal, non-commercial use provided that all copyright, trade and service marks and other proprietary notices are maintained. By accessing, sharing, receiving or otherwise using the Springer Nature journal content you agree to these terms of use (“Terms”). For these purposes, Springer Nature considers academic use (by researchers and students) to be non-commercial.
These Terms are supplementary and will apply in addition to any applicable website terms and conditions, a relevant site licence or a personal subscription. These Terms will prevail over any conflict or ambiguity with regards to the relevant terms, a site licence or a personal subscription (to the extent of the conflict or ambiguity only). For Creative Commons-licensed articles, the terms of the Creative Commons license used will apply.
We collect and use personal data to provide access to the Springer Nature journal content. We may also use these personal data internally within ResearchGate and Springer Nature and as agreed share it, in an anonymised way, for purposes of tracking, analysis and reporting. We will not otherwise disclose your personal data outside the ResearchGate or the Springer Nature group of companies unless we have your permission as detailed in the Privacy Policy.
While Users may use the Springer Nature journal content for small scale, personal non-commercial use, it is important to note that Users may not:

1. use such content for the purpose of providing other users with access on a regular or large scale basis or as a means to circumvent access control;
2. use such content where to do so would be considered a criminal or statutory offence in any jurisdiction, or gives rise to civil liability, or is otherwise unlawful;
3. falsely or misleadingly imply or suggest endorsement, approval , sponsorship, or association unless explicitly agreed to by Springer Nature in writing;
4. use bots or other automated methods to access the content or redirect messages
5. override any security feature or exclusionary protocol; or
6. share the content in order to create substitute for Springer Nature products or services or a systematic database of Springer Nature journal content.

In line with the restriction against commercial use, Springer Nature does not permit the creation of a product or service that creates revenue, royalties, rent or income from our content or its inclusion as part of a paid for service or for other commercial gain. Springer Nature journal content cannot be used for inter-library loans and librarians may not upload Springer Nature journal content on a large scale into their, or any other, institutional repository.
These terms of use are reviewed regularly and may be amended at any time. Springer Nature is not obligated to publish any information or content on this website and may remove it or features or functionality at our sole discretion, at any time with or without notice. Springer Nature may revoke this licence to you at any time and remove access to any copies of the Springer Nature journal content which have been saved.
To the fullest extent permitted by law, Springer Nature makes no warranties, representations or guarantees to Users, either express or implied with respect to the Springer nature journal content and all parties disclaim and waive any implied warranties or warranties imposed by law, including merchantability or fitness for any particular purpose.
Please note that these rights do not automatically extend to content, data or other material published by Springer Nature that may be licensed from third parties.
If you would like to use or distribute our Springer Nature journal content to a wider audience or on a regular basis or in any other manner not expressly permitted by these Terms, please contact Springer Nature at

onlineservice@springernature.com